

CHAPTER 1

INTRODUCTION

1.1 Statement and significance of the problem

Skin plays a significant biological role in maintaining health. The perception of what comprises “healthy” skin has strong psychological and social ramifications. After injuries, most wounds result in scars. Unfortunately, most scars are not functionally and cosmetically equivalent to the normal skin. The scars can contribute to low self-esteem, depression and social phobia. Morphologically, scars are divided into hypertrophic and atrophic varieties. Keloids and hypertrophic scars are characterized by excesses deposition of collagen in the dermis and subcutaneous tissues. They are raised, firm, shiny plaques that usually itch and are occasionally painful. Keloids and hypertrophic scars have the incident rate of about 4.5% to 16% of the general population (Kakar et al., 2006). The principles of managing of scars are to minimize collagen production and remove the collagenous nodules. The protease enzymes are widely used as meat tenderizing and defibrinating agents. These enzymes may have collagenolytic activity. Collagen degradation will result in the flatten and the reducible size of the collagenous nodules, thereby reducing the scar formation. Examples of the natural products which have been supported by several documented studies of having the protease enzyme activity are papain (the enzyme from the latex of the papaya fruit), and bromelain (the enzyme from the pineapple plant). These enzymes are macromolecules

which have the molecular mass of about 21-30 kDa. For keloids and hypertrophic scars application, the topical delivery of the protease enzyme is difficult not only from its molecule structure, but also the excessive accumulation of collagen of the scars which are the major barrier as well. Moreover, the protease enzyme will also be degraded by the epidermal enzymes. Thus, low percutaneous penetration and poor therapeutic effectiveness are usually obtained. The transdermal delivery of many pharmaceuticals of peptides and proteins faces enormous challenges, especially for the non-invasive treatment of both localized and systemic diseases.

Among several strategies, one of the most simple and convenient approach is the application of nanocarriers (nanobilayer vesicles or nanoparticulate systems). Niosomes, non-ionic surfactant vesicles, are microscopic lamellar structures formed on admixture of non-ionic surfactants and cholesterol in an aqueous media resulting in the closed bilayer structures. Niosomal structures are analogous to liposomes and are able to encapsulate aqueous solutes and serve as drug carriers. They have all the advantages of liposomes, with their superior low cost, greater stability, and ease of storage. So, they are now widely studied as an inexpensive alternative to liposomes or perhaps as the carrier systems, physically similar to liposomes. However, the conventional bilayer vesicles are not efficient to deliver transdermally across the skin, but rather remain confine to the upper layer of the stratum corneum. The more sophisticated bilayer vesicular formulations that can rapidly pass through the stratum corneum and remains in the deepest layer of the skin will be advantageous for the keloid and hypertrophic scar treatment. Currently, a bilosome which is a sophisticated lipid vesicle containing bile

salts has been developed. Nanoparticulate systems including nanospheres and nanocapsules which are submicron colloidal systems and have the mean particle diameter of 0.003-1 μm have been applied for topical use. The nanospheres prepared from poly (lactide-co-glycolide) (PLGA) are safe for human because of their biodegradability. They can also increase the shelf-life, protect from degradation and control the release over a longer period of time of the loaded substances (Vilaa et al., 2002; Rahimnejad et al., 2009). In this study, the natural peptides having collagen degradation activity were selected and loaded in nanocarrier formulations for scar treatment. The results from this study will obtain a novel efficient transdermal delivery system for the natural peptides for the treatment of keloids and hypertrophic scars.

1.2 Objectives

The purpose of this study was to develop an optimum nanocarrier formulation loaded with the peptide enzymes which were papain and bromelain for scar treatment. The best formulation with high physico-chemical stability during storage, high percentage of entrapment efficiency, proper transdermal absorption across the rat skin, high collagen degradation stimulation on human skin fibroblast *in vitro* or animal model was developed.

1.3 Scope of study

This study was divided into 6 parts which were the followings:

Part 1 : Development of the proper elastic niosomal formulations loaded with the model drug (calcitonin) by the chloroform film method with sonication

1.1 Effects of niosomal concentrations and various dispersants on physical characteristics of elastic niosomes

1.2 Effects of dispersants on the maximum loading and entrapment efficiency of calcitonin in elastic niosomes

1.3 Effects of phosphate buffer concentrations on physical characteristics of elastic niosomes

1.4 Comparison of physical characteristics and cytotoxicity of elastic niosomes containing ethanol and elastic niosomes containing the edge activators (NaC and NaDC)

Part 2 : Chemical stability and transdermal absorption of elastic niosomes loaded with the model drug (calcitonin)

2.1 Determination of the physical and chemical stability of the developed elastic niosomal formulations

2.2 Transdermal absorption of calcitonin loaded in elastic niosomes by vertical Franz diffusion cells

2.3 Selection of the best elastic niosomal formulation for loaded with protease enzymes

Part 3 : Preparation and biological activities of the extracted protease enzymes

3.1 Preparation of the crude extracts containing protease enzymes which are papain from papaya latex and bromelain from pineapple juice by precipitation

3.2 Qualitative and quantitative analysis of the protease enzymes by high performance liquid chromatography (HPLC) and sodium dodecyl sulfate polyacrylamide gel electrophoresis (SDS-PAGE) analysis

3.3 Investigation of the biological activities of the crude extracts containing protease enzymes including free radical scavenging activity, lipid peroxidation inhibition activity, human skin fibroblast cytotoxicity by SRB assay and gelatinolytic activity (zymography) on MMP-2

Part 4 : Preparation of blank elastic niosomes and NaC elastic niosomes loaded with the enzymes (papain and bromelain)

4.1 Determination of the physical characteristics of niosomal formulations

4.2 Investigation of the maximum loading and entrapment efficiency of the enzymes loaded in NaC elastic niosomes by gel filtration

4.3 Cytotoxicity and gelatinolytic activity (zymography) on MMP-2 stimulation on human skin fibroblasts of the enzymes loaded in NaC elastic niosomes

4.4 Determination of physico-chemical stability of the enzymes loaded in NaC elastic niosomes

Part 5 : Preparation of papain loaded nanospheres by the emulsion solvent diffusion methods in water (ESD) and the w/o/w emulsion solvent evaporation method (ESE)

5.1 Analysis of physicochemical properties of the papain loaded nanospheres such as particle size, zeta potential, morphology and encapsulation efficiency

5.2 The release profile of papain from the PLGA nanospheres

5.3 Cytotoxicity on human skin fibroblasts of papain loaded in PLGA nanospheres

5.4 Determination of physico-chemical stability of papain loaded in PLGA nanospheres

Part 6 : Development of gel containing papain loaded in nanovesicles and nanoparticles preparation for scar treatment

- 6.1 *In vitro* rat skin transdermal absorption by vertical Franz diffusion cells
- 6.2 Investigation of rabbit skin irritation test by the closed patch test
- 6.3 Determination of the physico-chemical stability of gel containing papain loaded in nanovesicles and nanoparticles
- 6.4 *In vivo* hypertrophic scar model in the rabbit ears

1.4 Literature reviews

1.4.1 Wound and scar

After tissue injury by trauma, surgery or inflammation, the body attempts to repair the damage tissue. The wound healing process is divided into three phases which are inflammatory, proliferative and remodeling (**Figure 1**). First, the inflammatory phase, it occurs immediately after injury which is marked by platelet accumulation, coagulation, migration of inflammatory cells such as neutrophils, leukocytes and macrophages to the wound from surrounding blood vessels and the release of mediators and cytokines. Second, the proliferative phase which is characterized by promoting the granulation tissue formation which consists of re-epithelialization, fibroplasia and angiogenesis. Third, the new collagen matrix becomes cross-linked and organized for remodeling. In normal scar maturation, this phase results in a balance between the synthesis and degradation of collagen and regression of the stimulatory factors. Unfortunately, most wounds are not functionally equivalent to the normal skin and results

to be a scar. Scars are categorized into two main groups. They are scars involving tissue loss (atrophic) and scars involving tissue excess (hypertrophic).

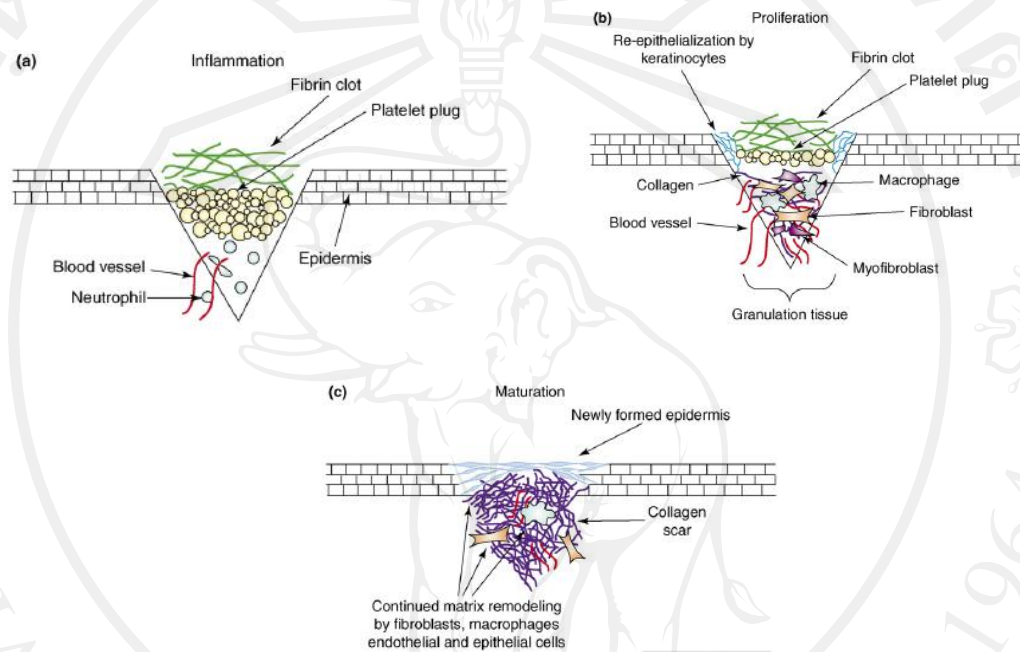


Figure 1 The phase of wound healing can be divided into 3 phases: inflammation (a), followed by proliferation (b) and lastly the ongoing process of scar maturation (c) (Rhett et al., 2008).

1.4.1.1 Pathophysiology of hypertrophic scars and keloids

Keloids and hypertrophic scars are from skin alteration due to injuries.

They are cutaneous abnormalities that are characterized by the excessive accumulation of extracellular matrix (ECM) protein, especially collagen. Several documents have studied the biochemical composition of the scars (Abergel et al., 1985; Meenakshi et al., 2005). Both keloids and hypertrophic scars have excess collagen and proteoglycans, a higher

amount of acid-soluble collagen and water content than the normal skin. The rate of proliferation and metabolic activity of keloid fibroblasts are more than hypertrophic scars and normal skin fibroblasts. So, keloids can extend beyond the borders of the original wound and spreads by invasion rather than expansion. Hypertrophic scars remain confined to the borders of the original wound and most of the times retain their shape. The previous study has found some differences in the organization of the connective tissue and cell between keloids and hypertrophic scars (Santucci et al., 2001). Keloids presented large collagenous nodules and haphazardly orientation of collagen bundles and fibers. Hypertrophic scars presented a high number of spindle-shaped cells (α -smooth muscle actin) which are absent from keloids. The mechanism of keloid and hypertrophic scar forming are not fully understood. These scars seem to function autonomously. There is the loss of the normal control mechanisms, resulting in an increase in the production of fibroblastic collagen and matrix metalloproteinase (Fujiwara et al., 2005) and a decrease in collagen degradation (Wu et al., 2002). There are many hypothesis of pathologies of keloids and hypertrophic scars. The excess collagen production can be attributed to high level of nitric oxide, the free radical which will stimulate the fibroblast to synthesize collagen (Cobbold, 2001). The mechanical loading early in the proliferative phase of wound healing produces keloids and hypertrophic scars by inhibiting cellular apoptosis (Aarabi et al., 2007).

1.4.1.2 Treatment of scars

There are two methods of treating elevated scars as the followings:

A. Invasive treatment (Mutalik, 2005)

This includes surgery, radiation therapy, steroid injections, cryotherapy (treatment with liquid nitrogen) and laser therapy. Intralesional corticosteroid is widely used but has complications (fat atrophy, dermal thinning and pigment changes). Other treatments have been advocated with variable outcomes include injections of fluorouracil, interferon gamma and bleomycin. These treatments require specialists and are uncomfortable. Moreover, side effects have been reported such as extreme pain and high recurrence rate.

B. Non-invasive treatment (Zurada et al., 2006)

The non-invasive scar treatment becomes increasingly popular because of their ease and comfort use, non-invasiveness and relatively low cost. The examples of topical therapies including pressure therapy or compression garments are preferred for treating the scars after burn injury. Treatments with topical products containing agents that can inhibit collagen production or stimulate collagen degradation activity appear to be the easy and good approach for the exposed areas. These agents include imiquimod, retinoic acid (vitamin A), tocopherol (vitamin E), mucopolysaccharide polysulphate (MPS) and the onion extract. Currently, these agents have unclear effects on the keloids and hypertrophic scars. Thus, to find a new agent for treating scar is interesting and challenging.

1.4.1.3 Pharmacologic therapies of hypertrophic scars and keloids

There is no universal treatment for abnormal scars. Formation prevention of a poor or abnormal scar is the primary treatment to be considered. Most

unsatisfactory scars should be left alone for at least one year to allow scar maturation before a decision is made for the treatment. Patients should be informed and shared in the decision-making process to avoid unrealistic expectations. Many pharmacologic agents have been used to modulate the wound healing and scar formation process. **Table 1** showed various studies on the therapies and their proposed mechanisms for wound healing and scar formation.

1.4.1.4 Scar treatment products available in the markets

Many products for scar reduction have been launched in the markets in order to supply the demand of the patients as shown in **Table 2**.

1.4.2 Natural peptides

Most consumers believe that the natural products are devoid of irritants and chemically hazardous materials. Peptides play a vital role in all biological process and have received a growing attention in the recent years as drug candidates. For examples, bacitracin is a polypeptide antibiotic produced by *Bacillus subtilis* var Tracy and is used as a topical treatment for bacterial infections. Insulin is a protein in human body that plays a major role in decreasing the levels of blood glucose and regulating the metabolism of glucose, fats and proteins. Many natural agents have been used to treat scars, such as Guta Kola extract (*Centella asiatica* (Linn.) Urban), onion extract (*Allium ascalonicum* Linn.) and protease or collagenase enzymes from bacteria (*Clostridium histolyticum*) as well as many herbs.

1.4.2.1 Sources of natural peptides

Peptides, a group of compounds consisting of two or more amino acids linked by the peptide bond, and are abundantly present in living organisms. Thousands of peptides have been isolated from animals, plants and microorganisms. There are many researches on the peptides from natural sources. The previous study has prepared the angiotensin converting enzyme (ACE) inhibitory peptides from the Silver carp (*Hypophthalmichthys molitrix*) using protease hydrolysis. The ACE inhibitory activity of the five proteases was ranged from 10.27 to 88.08% (Jin-Chao et al., 2011). Longicalycinin A, new cyclic peptide which isolated from the methanolic extract of *Dianthus superbus* var. longicalycinus has been reported to be active against HepG2 cancer cell lines with an IC₅₀ value of 13.52 µg/ml (Hsieh et al., 2005). The crude extract from the culture of *Pseudoalteromonas* sp. associated with the Thai sponge *Halisarca ectofibrosa* having the six peptides (cyclo-[leucyl-prolyl]₂, cyclo-[phenylalanyl-prolyl]₂, cyclo-[prolyl-leucyl-phenylalanyl-leucyl]₂, cyclo-[prolyl-leucyl-alanyl-isoleucyl]₂, cyclo-[phenylalanyl-leucyl]₂ and cyclo-[leucylisoleucyl]₂) was found to inhibit the growth of *Bacillus subtilis* and *Vibrio anguillarum* (Rungprom et al., 2008).

1.4.2.2 Applications of natural peptides

Nature has developed a vast number of peptides in all living and the past species that display an exceeding diversity of structure and biological effects. In recent years, natural peptides have been used as various pharmaceutical products. For example, peptic digestion of the porcine skeletal muscles has resulted in the generation of numerous ACE inhibitory peptides. Glu-Lys-Glu-Arg-Glu-Arg-Gln (EKERERQ) and





Table 1 Various studies on the treatment approaches and their proposed mechanisms of wound healing and scar formation

Treatments	Mechanisms of action	Examples of the study
Excision	Surgical removal of scar	Recurrence rate for surgery alone ranged from 45-100% (Mustoe et al., 2002).
Radiation	Apoptosis of proliferating cells in scar tissue	147 keloids were surgically removed, and the patients were treated postoperatively with 15-Gy electron-beam irradiation and followed for more than 18 months. The overall recurrence rate was 32.7% (Ogawa et al., 2003).
Laser	Induces tissue hypoxia and decreased cellular function; disrupts disulfide bonds leading to fiber remodeling; collagenolysis following cytokine stimulation	A recent study of 22 female subjects who underwent PDL scar excision showed substantial clinical (increased pliability and decreased pruritus) and histological (decreased sclerosis) improvement (Alster, 2003).
Cryotherapy	Induces vascular damage and circulatory stasis, thrombosis, and transudation of fluid leading to anoxia and eventual necrosis	An average of 51.4 percent of scar volume reduction was achieved after one session of intralesional cryosurgery treatment (Har-Shai et al., 2003).
Triamcinolone acetonide	Inhibits α 2-macroglobulin (inhibits collagenase breakdown of collagen); decreases production of TGF- β 1	Keloids treated by injecting triamcinolone acetonide at 4 week intervals. Improvement in subjective symptoms was seen in 82% and in objective symptoms, fair results were in 63%, and good results in 39% (Muneuchi et al., 2006).
Pressure garments/devices	Decreases α -macroglobulins; scar hydration; mast cell stabilization; tissue ischemia; release of metalloproteinase-9 or PGE2, which induces extracellular matrix remodeling	The recommendation for external ear keloid therapy is to maintain the pressure at 24-30 mmHg, and the duration of the form-pressure therapy was about 25 weeks (Chrisostomidis et al., 1998).
Silicone gel dressing	Increased pressure on wound; hydration of the stratum corneum; silicone gel increases the temperature of the scar, possibly increasing collagenase activity	The scar elevation index was significant reduced after 4 week application of silicone gel versus untreated (1.15 ± 0.15 versus 1.71 ± 0.33 , respectively; $P < 0.001$) (Saulis et al., 2002).

Table 1 Various studies on the treatment approaches and their proposed mechanisms of wound healing and scar formation (continued)

Treatments	Mechanisms of action	Examples of the study
Onion extract	Stabilizes mast cell membranes causing reduced histamine release and decreased collagen production	Topically applied onion extract in gel for 6 months was more effective in relation to scar color. However, it was ineffective in improving scar height and itching (Hosnuter et al., 2007).
Retinoic acid	Inhibitory effect on DNA synthesis in lymphocytes and fibroblasts <i>in vitro</i>	A statistically significant 20% reduction in scar size in the 0.05% retinoic acid treatment group compared with the base cream control group (Daly et al., 1986).
Imiquimod	Stimulates immune pathways enhancing healing ability; induces local synthesis of cytokines causing down-regulation of collagen synthesis	Apply imiquimod 5% cream on the wound area 2 weeks after the operation could effectively prevent recurrence of the excised keloids, especially in the area that had less tension such as pinna (Chuangsuwanich et al., 2007).
Antioxidants	Inhibits scar fibroblast proliferation, contraction, and production of collagen	Topically applied vitamin E does not help in improving the cosmetic appearance of scars and leads to a high incidence of contact dermatitis (Baumann et al., 1999).
Fluorouracil	Inhibits fibroblast proliferation by blocking DNA synthesis and transcription through competitive inhibition of thymidylate synthesis	In a prospective, randomized trial including 28 consecutive patients with keloids of varying size and duration, weekly intralesional 5-FU injections (50 mg/ml) for 12 weeks resulted in reduction in scar size of at least 50% in the majority of the patients (Nanda et al., 2004).
Bleomycin sulfate	Inhibits TGF- β stimulated collagen synthesis in skin fibroblasts	After treated with bleomycin tattoo for 1-month period in 45 patients, the therapeutic response was higher than 88% of the keloids (Naeini et al., 2006).
Interferon	Inhibits types I and III collagen synthesis via reduction in cellular messenger RNA	Hypertrophic scars injected three times weekly with IFN- α 2b showed significant mean rates of improvement and sustained reduced serum TGF- β levels (Tredget et al., 1998).

Table 2 The examples of the scar reduction products available in the markets

Types	Products	Features	Appearances of the products
Silicone gel sheets	Cica-Care gel sheeting (Smith and Nephew, Largo, Fla)	Thin, self-adhesive, flexible gel sheets	 <p>http://www.alldaymedical.com/images/prodimages/SN66250707_PL.jpg</p>
Polyurethane dressing	Cutinova thin dressing (Smith and Nephew)	Self-adhesive, flexible, breathable, semitransparent pads; maintain a moist wound environment and help prevent bacterial contamination	 <p>http://www.cenmedonline.com/productImages/BE47578.jpg</p>
Onion extract	Mederma (Merz Pharmaceuticals, Greensboro, NC)	Greaseless, pleasant-smelling clear gel; new separate kid-friendly preparation	 <p>http://www.vatgia.com/raovat_pictures/11/larger_won1307794861.jpg</p>
Imiquimod 5% cream	Aldara (3M Pharmaceuticals Pty Ltd)	Pleasant-smelling cream	 <p>http://www.buyersguide.com/images/Genital Warts/GracewayPharmaceuticalsAldara.jpg</p>

Lys-Arg-Gln-Lys-Tyr-Asp-Ile (KRQKYDI) were identified as the active peptides, and their 50% inhibitory concentrations were found to be 552.5 and 26.2 μM , respectively (Katayama et al., 2008). Some peptides from the marine plants also exhibited the potential antitumor activities. Two cyclopeptides from *Lyngbya semiplena* have been found to have significant cytotoxic effects in the NCI-H460 cell line of human lung tumor and neuro-2a murine neuroblastoma cell lines. The IC_{50} for both tumor cells was 0.4 $\mu\text{mol/l}$ (Han et al., 2005). The peptide seed extract of Bitter gourd (*Momordica charantia*), contained alpha- and beta-momorcharins which was efficient against *Staphylococcus aureus* and *Salmonella typhi* with the maximum zone of inhibition (1 cm) in comparing to the chloramphenicol which showed the clear zone of 2 cm (Mahmood et al., 2012).

In addition, some peptides from natural sources exhibited antioxidative activity which can be used in cosmeceutical products. Antioxidant peptides have been found in numerous foodstuffs including milk, wheat, potato and fungi. Seven antioxidant peptides were identified in the hydrolysates of proteins recovered from the waste stream of sardinelle processing. The amino acids sequences were LARL, GGE, LHY, GAH, GAWA, PHYL and GALAAH (L=leucine, A=alanine, R=arginine, G=glycine, E=glutamic acid, H=histidine, Y=tyrosine, W=tryptophan and P=proline). It was reported that the peptide LHY displayed the highest DPPH radical scavenging activity, with an ability to scavenge 63% of the available DPPH radical present at the peptide concentration of 150 $\mu\text{g/ml}$ (Bougatef et al., 2010). The tripeptide (glycyl-L-histidyl-L-lysine) complexed with copper (Cu-GHK) which was isolated from the albumin fraction

of the human serum have been shown to promote new blood vessel growth, enhance the expression of the growth factors and stimulate the formation of new collagen, elastin and glycosaminoglycan components of the tissue to accelerate the repair process. The combinative stimulation for *in vitro* collagen production (when photoirradiation was followed by Cu-GHK-supplied incubation) showed increased bFGF secretion, procollagen type I C-peptide production and type I collagen expression compared to the photoirradiation treatment alone (Huang et al., 2007).

1.4.2.3 Protease enzymes

Protease enzymes also refer to proteolytic enzymes and proteinases. They are the degrade proteins by hydrolyzing the peptide bond. Proteases can either break the specific peptide bonds called the limited proteolysis, or break down the complete polypeptide chain to the amino acid residues.

A. Classification of the protease enzymes

Proteases are classified into six groups which are serine proteases, threonine proteases, cysteine proteases, aspartic acid proteases, metalloproteases and glutamic acid proteases (Polaina et al., 2007). From the different types of proteases, alkaline proteases are one of the most widely studied groups of enzymes because of their wide use in many industrial applications including food, leather, pharmaceutical and detergent industries. The cysteine proteases can be subdivided into exopeptidases (e.g. cathepsin X, carboxypeptidase B) and endopeptidases (e.g. papain, bromelain, ficain). Exopeptidases can cleave the peptide bond proximal to the amino or carboxy terminal of the substrate, whereas endopeptidases can cleave

peptide bonds distant from the N- or C-terminal. The role of cysteine proteases is crucial in normal cellular metabolism, being fundamental to intracellular protein turnover, degradation of collagen and cleavage of precursor proteins.

B. Sources of protease enzymes

The world market for enzymes grows 7.6% per year and will reach \$7 billion in 2013. Protease enzymes account for nearly 65% of the industrial enzyme market in the world. The major source of proteases are microorganisms such as *Bacillus subtilis megatherium* (Gerze et al., 2005), *Pennicillium chrysogenum* (Haq et al., 2006) and *Tannerella forsythia* (Kawase et al., 2010). The protease of *Taenia solium* metacestodes could degrade human immunoglobulin G (IgG), collagen and bovine serum albumin (BSA), but human IgG was more susceptible for proteolysis (Kim et al., 2005). Another source of proteases is from plants which governed by several factors such as the availability of land for cultivation and the suitability of climatic conditions for growth. However, proteases from plants are lack of hypersensitivity which is different from those from microorganisms. Proteases have been identified and studied from the latex of several plant families such as *Asteraceae*, *Caricaceae*, *Moraceae*, *Asclepiadaceae*, *Apocynaceae* and *Euphorbiaceae* (Domsalla et al., 2008). The cysteine protease from ginger had the high proteolytic activity against undefined substrates such as casein, bovine serum albumin and collagen (Hashimoto et al., 1991).

C. Scar treatment by protease enzymes

Protease enzymes have been used in several therapeutic properties including cleaning wounds from necrotized tissue (Mahmood et al., 2005;

Tochi et al., 2008), accelerating post-operation scar tissue resorption and debriding small residual traces (hypertrophic and keloid scars) after plastic operations (Pendzhiev, 2002), preventing aggregation of human blood platelets (Tochi et al., 2008) and proteolysis of collagen (Thompson et al., 1973). Moricrase was the complex of collagenolytic and fibrinolytic proteases. It was isolated from the king crab (*Paralithodes camchatica* hepatopancreas). A partial removal of necrotic debris, the formation of red granulation tissue, and the beginning of wound edge re-epithelialization were observed on day 3 after a single application of Moricrase to rat purulent wounds. Complete debridement was observed as early as day 10. Moricrase-containing ointment was tested in reconstructive surgery. The conservative treatment was carried out with patients having post-traumatic and post-operative scars (**Table 3**). No side effects were observed after ointment application during 1-3 months. Collagenolytic activity of Moricrase has been used in medical applications in the treatment of ulcers and scars (Rudenskaya et al., 2000).

Table 3 Effect of Moricrase-containing ointment application on keloid scars
(Rudenskaya et al., 2000)

Scar tissue	Total amount of patients	Considerable effect	Moderate effect	No effect
Keloid scar:				
Posttraumatic	17	12	2	3
Postoperative	15	10	5	-
Hypertrophic	7	5	2	-

^aConsiderable effect: reddening and itch of scar tissue were decreased, the scar became more plane and soft.

^bModerate effect: reddening and itch of scar tissue were decreased, but the softening of the scar was not observed.

1.4.3 Papain

Carica papaya L. belongs to the small family Caricaceae. It is actually large herb growing to 16-33 feet height with a single stem. The tree is usually unbranched and unless lopped. The leaves are large (50-70 cm diameter) and deeply palmate lobe with 7 lobes. Papaya flowers have five cream-white to yellow-orange petals 2.5-5.1 cm long. The stigmatic surfaces are pale green, and the stamens are bright yellow. The fruits are smooth skinned and contain many seeds (**Figure 2**).

1.4.3.1 Protease enzymes from papaya

The presence of protease enzymes in fresh latex from both the fruits and the plant vegetative organs such as stems, petioles, and leaves has been reported. The crude latex of papaya fruit contains the mixture of cysteine proteases including papain, chymopapain, glycyl endopeptidase and caricain. These enzymes have more than



Figure 2 Papaya tree and fruit (*Carica papaya* L)

http://upload.wikimedia.org/wikipedia/commons/8/84/Carica_papaya_

[_K%C3%B6hler%E2%80%93Medizinal-Pflanzen-029.jpg](#)

80% of the whole enzyme fraction. Papain is the best known protease enzyme which is isolated from the fruits of papaya (*Carica papaya*). It is a polypeptide chain composing of 212 amino acids with the molecular weight of 23.4 kDa. Papain contains the sulfhydryl group at the active site which is located at the 25th amino acid and creates the small loop in the molecule involving the next approximately 30 amino acids. The remaining sulfides of the enzyme are found on three distinct disulfide bridges which are important to the structure folding. Papain is completely soluble in water (10 mg/ml) but insoluble in alcohol. It is relatively basic protein, with the isoelectric point of 8.75, having an optimum catalytic activity at pH 5-8.

1.4.3.2 Methods of extraction and purification

There are several methods to separate papain from the papaya latex including salt precipitation, aqueous/solvent extraction and cation exchange chromatography.

A. Salt precipitation

Traditionally, papain is purified by multi-steps salt precipitation followed by crystallization. However, the process is time-consuming and the purified enzyme still contaminated with other proteases. Previous research showed that the two-step precipitation method can be used for purification of papain. The first precipitation was performed using ammonium sulfate while sodium chloride was used for the second precipitation step. The maximum purity of papain (89%) was achieved during the second precipitation to 6 mg/ml (Nitsawang et al., 2006).

B. Aqueous/solvent extraction

Papain has been extracted by the precipitate with organic solvents. This method is the simple method which is the cost- and time-saving extraction process. The precipitation of protease from papaya peels with 70% (v/v) ethanol provided the highest proteolytic activity of 57.61% (Chaiwut et al., 2007). The aqueous two-phase systems (ATPS), made up of two polymers or one polymer and a salt in water, have shown interesting potential for downstream processing of proteins extraction. They have been successfully applied for large-scale enzyme separation and purification. The purification of papain by the aqueous two-phase system provided high recovery of 88% with purity of 100% (Nitsawang et al., 2006).

C. Ion exchange chromatography

The alternative purification strategy has involved the use of various chromatographic techniques including ion exchange, covalent or affinity chromatography, but it is difficult to scale up and the cost is high. Chromatography on cation-exchange supports has been used as the first purification step of the papaya enzymes (Azarkan et al., 2003). The elution pattern was obtained at pH 5.0 on the SP-Sepharose Fast Flow. Protein fractions from the cation-exchange supports were generally regrouped into four pools. The second pool (denoted PAP in **Figure 3**) contains papain as the main constituent.

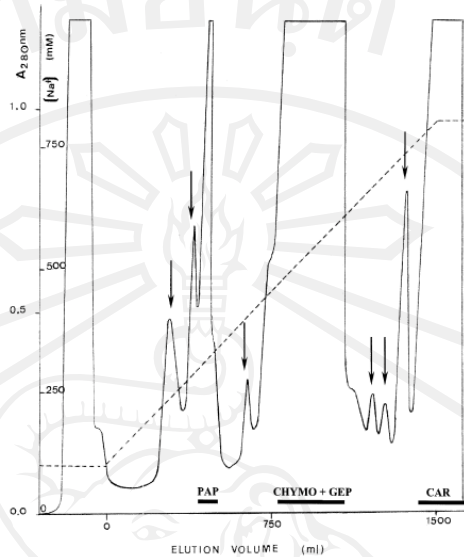


Figure 3 Ion-exchange chromatography of the papaya enzymes on the SP-Sepharose Fast Flow. The solid bars indicated the fractions that were pooled for poly (acrylamide) gel analysis (Azarkan et al., 2003).

1.4.3.3 Qualitative and quantitative analysis of papain

A. Electrophoretic method

The enzyme fractions from the papaya latex obtained by column chromatography were analyzed by electrophoresis, which was the main method used for the investigation of proteins. This method has been considered as a good analytical technique to resolve and separate the individual components of protein mixtures. It was able to characterize proteins in terms of their molecular size. The analysis was performed on the poly(acrylamide) gel (PAG) containing 15% of acrylamide. The PAG electrophoresis was conducted in acid solutions (pH 4.5) at an

applied voltage of 250 V and a current of 45 mA. As can be seen in the pattern presented in **Figure 4**, the band of papain appeared on the gel (arrow no.1 in lane c).

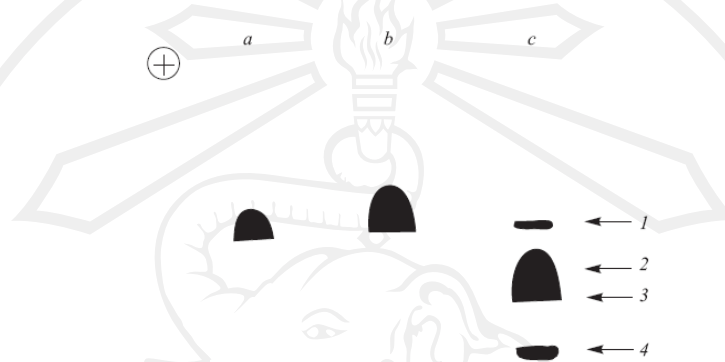


Figure 4 The PAG electrophoresis patterns of (a) proteinase obtained by affinity chromatography on the immobilized cystatin, (b) reference papain (Serva), and (c) *Carica papaya* latex sample: (1) papain; (2) chymopapain; (3) peptidase B; (4) peptidase A (Pendzhiev, 2002).

B. High performance liquid chromatography (HPLC) (Kumar et al., 2005)

The previous study has analyzed papain purity by Rp-HPLC. The mobile phase used was 0.1% trifluoroacetic acid (TFA, Solvent I) and 70:30 acetonitrile: water containing 0.05% TFA (Solvent II). Papain was dissolved in distilled water and loaded onto a Shimpak octadecylsilane (ODS) column (250 x 4.5 mm) previously equilibrated with the mobile phase (Solvent I). The column was washed by the gradient run consisting of 0% solvent II traversing to 100% in 90 min at a flow rate of 1.0 ml/min. The elution was monitored at 280 nm. The appearance of a single peak on

Rp-HPLC confirmed its purity (**Figure 5**). In addition, N-terminal sequence analyse of papain was found to be Ile-Pro-Glu-Tyr-Val-Asp-Try-Arg-Glu-Lys by Applied Biosystem Protein Sequenator (Model 789, USA).

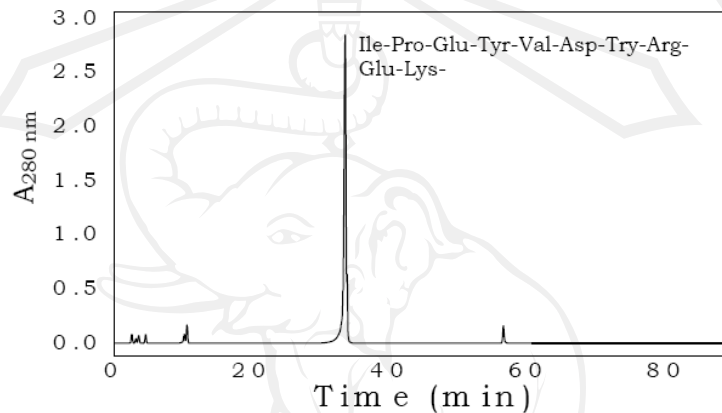


Figure 5 Rp-HPLC profiles of papain (Kumar et al., 2005)

C. Immunoassay technique

Immunoassays are preferred for the quantitative of many clinically relevant analytes. The high binding affinities and the specificity of analyte recognition displayed by antibodies greatly simplify the accurate determination of analytes, despite the presence of many other substances in a sample of interest. An antibody raised to papain has been used in the development of an enzyme-linked immunoabsorbent assay (ELISA) for the determination of papain in raw meat. Quantitative determination of papain up to 4 mg/kg of raw meat has been obtained using standard extracts prepared by the exogeneous addition of papain to raw beef. A sample of commercially treated ‘tenderised beef’ was shown to contain papain at the level of 0-40 mg/kg (Sargeant et al., 1993). ELISA has been applied to estimate the encapsulation

efficiency of papain in microspheres. The microspheres were dissolved in ethanol-phosphate buffer (pH 7.4) mixture (1:1). The resulting solution was analyzed for papain content by measuring absorbance in an ELISA at 540 nm using Micro BCA™ protein assay kit (Sharma et al., 2011).

1.4.3.4 Papain in pharmaceutical and cosmeceutical applications

A. Pharmaceutical applications

The proteolytic and antiinflammatory properties of papain allow it to be applied in surgery for the treatment of various fistulas, cleaning wounds from necrotized tissues, and preparing trophic ulcers for skin grafting (epidermatoplasty).

It has administrated oral therapy with the protease enzymes containing papain in patients with rheumatoid arthritis (n=38), osteomyelofibrosis (n=7), herpes zoster (n=7), and in seventy-eight healthy volunteer control group and observed statistical decreases in serum levels of TGF-β1 (transforming growth factor beta 1). It has been demonstrated that protease enzymes reduce TGF-β levels in serum by converting the protease inhibitor α2 macroglobulin (α2 M) (Desser et al., 2001). Papain exhibited remarkable mycelia inhibition with mean zones of inhibition at 1.20, 0.67 and 0.34 mm for *Aspergillus Niger*, *Mucor* spp. and *Rhizopus* spp., respectively (Chukwuemeka et al., 2010).

B. Cosmeceutical applications

Enzymes are one of the potential active ingredients in cosmeceutical products. Papain can hydrolyze the peptide bonds of collagen and keratin in the stratum corneum of the skin. The controlled skin damage can then trigger skin repair and bring to the surface the layer of smoother and softer skin. Papain has

advanced exfoliation effects upon the stratum corneum. Lotion containing 1% papain conjugate with SC-glucan was more effective in exfoliating stratum corneum of skin than the lotion containing 5% lactic acid with no sign of irritation such as redness (Sim et al., 2000). The previous study has assessed the antioxidant potential of the juices of 3 papaya cultivars (PCJ including Sunrise Solo, Red Lady, and Tainung). The IC_{50} values of Sunrise Solo (52.1 ± 1.5 ml PCJ/g DPPH) was better than that of the Red Lady (63.4 ± 2.9 ml PCJ/g DPPH) and Tainung juices (71.8 ± 1.8 ml PCJ/g DPPH). PCJ showed a linoleic acid peroxide scavenging activity that was 5 times higher (during 72 h) than in the negative control, but close to that of vitamin E (Özkan et al., 2011).

1.4.3.5 Papain in scar treatment

In surgical cosmetology, papain is used for accelerating post-operation scar tissue resorption and debriding small residual traces (hypertrophic and keloid scars) after plastic operations. The aqueous extract of papaya fruit (100 mg/kg/day) promoted significant wound healing in diabetic rats. The extract-treated rats exhibited 77% reduction in the wound area when compared to controls which was 59%. The extract treated wounds were found to epithelize faster as compared to the controls (Nayak et al., 2007). Rats treated with papain-based wound cleanser showed a progressive wound healing based on the wound reduction rates and histological analysis when compared with rats treated with distilled water and Betadine. Better collagen deposition and presence of skin organelles in rats treated with papain-based wound cleanser demonstrated its efficacy in promoting wound healing (Ajlia et al., 2010). The topical application of papaya latex showed wound healing properties in mice burn model. Gel

containing dried papaya latex significantly increased hydroxyproline content. Significant percentage wound contraction was observed from day 12 in the 2.5% papaya latex and from day 20 in the 1.0% papaya latex. The epithelialization time of the 2.5% papaya latex (22 ± 0.57 days) was found to be the shortest, while the epithelialization time of control (no treatment) mice was 32 ± 0.66 days (Gurung et al., 2009).

1.4.4 Bromelain

Bromelain is a complex mixture of proteases typically derived from the ripe and unripe fruits, as well as the stems and leaves of Pineapple plant (*Ananas comosus*). Pineapple is the common name for an edible tropical plant and also its fruit. It is a herbaceous perennial which grows to 1-1.5 m tall. The plant has a short, stocky stem with tough and waxy leave to 1.5 m long, 1.5 cm wide. Its flower with violet petals and fruits held erect on the stout scape, large and succulent (**Figure 6**).



Figure 6 Pineapple plant and fruit (*Ananas comosus*)

1.4.4.1 Protease enzymes from pineapple

The pineapple plants contain at least four distinct protease enzymes.

Table 4 showed the characteristics of the protease enzymes from the pineapple plants. The major endopeptidase presents in the extracts of the plant stem is termed "stem bromelain", whereas the major enzyme fraction found in the juice of the pineapple fruit is named "fruit bromelain". Some other minor cysteine endopeptidases (ananain, comosain) are also found. The term "bromelain" can refer to the combination of four enzymes along with other compounds produced in an extract such as phosphatases, glucosidases, peroxidases, cellulases, glycoproteins and carbohydrates.

Table 4 Characteristics of protease enzymes from pineapple (Maurer, 2001).

Name Reference (EC number)	Molecular mass (Dalton)	Isoelectric point	Sequences	Glycosylation
Stem bromelain (EC 3.4.22.32)	23,800 (sequence+sugar)	>10	completely sequenced (212 amino acids)	glycosylated
Ananain (EC 3.4.22.31)	23,464 (sequence)	>10	completely sequenced (216 amino acids)	not glycosylated
Comosain	24,509 and 23,569 (esms)	>10	N-term. Sequence	glycosylated
	23,550 and 23,560 (esms)	4.8 and 4.9	N-term. sequence	highly glycosylated
Fruit bromelain (EC 3.4.22.33)	23,000	4.6	N-term. sequence	not glycosylated

The approximate molecular weight of bromelain is about 23-25 kDa. Bromelain has high activity at an optimum pH at 4.5-5.5. Bromelain is readily soluble in water, insoluble in most organic solvents such as acetone, ether, ethanol and methanol. Bromelain can be activated by calcium chloride, cysteine, bisulphate salt, NaCN, H₂S, Na₂S and benzoate. However, bromelain is usually sufficiently active without the addition of activators. Bromelain is inhibited by Hg²⁺, Ag⁺, Cu²⁺, antitrypsin, estatin A and B, iodoacetate. Fruit bromelain has much higher proteolytic activity in comparing to the stem bromelain and a broader specificity for peptide bonds (Hale et al., 2005). It may be from the different type of proteases which stem and fruit bromelain are cysteine and aspartic endopeptidase enzymes, respectively.

1.4.4.2 Methods of extraction and purification

Isolation, separation and purification of enzymes can be performed using by a variety of methods including chromatography, electrophoretic, ultrafiltration, precipitation and other procedures.

A. Precipitation method

The cost- and time-saving extraction process of bromelain is the traditional precipitation. Ethanol, ammonium sulfate and acetone have been widely used to extract bromelain from pineapple plants. Bromelain was precipitated with 30-70% ethanol of percentage yield 41.91%, which was achieved a purification factor of 2.34 (Soares et al., 2011). Bromelain extract which was purified by the 40-60% and 60-80% (w/v) saturated ammonium sulfate precipitation showed higher specific protease activity and protein contents than that from the same method but with other saturation

levels. The enzyme recovery and protein content were found to be about 80 and 34% of the total enzyme and protein contents, respectively (Devakate et al., 2009). Bromelain precipitated with 40-50 % acetone concentration showed the highest specific enzyme activity among other concentrations (Chen et al., 1972).

B. Aqueous two phase extraction

Aqueous two-phase system has been applied for several years as a good laboratorial separation technique and it can be used as a pre-purification step. This system has been tested with large success. It is formed by two aqueous phases immiscible or partially miscible within themselves, obtained by the addition of hydrophilic polymers or one hydrophilic polymer and a salt, such as the poly(ethylene glycol)-PEG and potassium phosphate salt systems. The polyethylene glycol/potassium phosphate system (comprising of 18% PEG1500 and 14% phosphate) increased the purity of bromelain about 4 folds and showed 228% activity recovery (Ravindra Babu et al., 2008). It has been reported that bromelain was extracted by the system composed of 18% PEG6000 and 17% $MgSO_4$ which increased purity of 3.44 folds with an activity recovery of 206% (Ketnawa et al., 2011).

C. Ion exchange chromatography

Ion exchange chromatography is often very useful in protein purification. This chromatographic procedure uses the net charges of the molecules to achieve their separation. Bromelain was partially purified using chromatography on the cation exchange chromatography CM Sphadex C-50 at pH 4.5 and gel filtration on Zorbax GF-250 (Agilent). The partial purification was successful and 5.6 fold

purification was achieved (Masdor et al., 2011). The high purity bromelain was obtained from the extract using cation exchange resin. The elution efficiency in chromatographic purification was obtained in the range of 80-90%. The fold purity obtained by chromatography was 3.3 times higher than that obtained by ammonium sulfate precipitation (Devakate et al., 2009).

1.4.4.3 Qualitative and quantitative analysis of bromelain

A. Electrophoretic method

The homogeneity of bromelain was confirmed by SDS-PAGE (sodium dodecylsulphate-polyacrylamide gel electrophoresis) analysis. The extracted enzymes were loaded onto a 3.5% stacking gel and subjected to electrophoresis on a 12% separating gel at 200 V. The bands of the enzymes which appeared in the gel were compared at the molecular weight (MW) with the protein marker. The SDS-PAGE analysis showed that extracted protein (bromelain) was represented in **Figure 7**. The estimated molecular weight of bromelain was around approximately 30 kDa (Gautam et al., 2010).

B. High performance liquid chromatography (HPLC)

Bromelain concentration was analysed using HPLC analysis.

Bromelain solution was loaded onto a TSK Gel column and eluted by buffer solution which contain 20 mM sodium phosphate and 0.5 M sodium chloride. The elution was monitored at 280 nm. The standard curve of bromelain standard was plotted and used as reference for bromelain quantification in the samples (Majid et al., 2008).

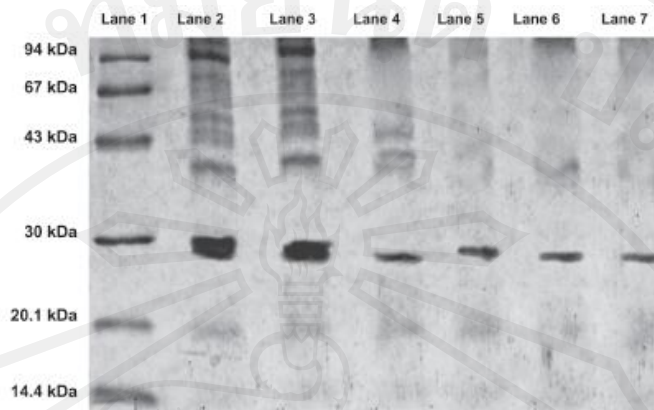


Figure 7 SDS-PAGE electrophoresis of isolated bromelain. Lane 1: standard of molecular weight, Lane 2: crude stem bromelain; Lane 3: crude fruit bromelain; Lane 4: 2nd eluate stem bromelain; Lane 5: 4th eluate stem bromelain; Lane 6: 2nd eluate fruit bromelain; Lane 7: 4th eluate fruit bromelain (Gautam et al., 2010).

C. Infrared (IR) spectroscopy

Infrared spectroscopy is one of the oldest and well established experimental techniques for the analysis of structure of polypeptides and proteins. It is convenient, non-destructive, requires less sample preparation, and can be used under a wide variety of conditions. IR spectroscopy is the measurement of wavelength and intensity of the absorption of IR radiation by substance. **Figure 8** showed the FTIR spectra of freeze-dried bromelain powder. The characteristic C-N stretch vibration frequencies of monoalkyl guanidinium were assigned to observed IR bands at 1655-1685, 1615-1635 and 1170-1180 cm^{-1} . The band at 1630-1860 cm^{-1} showed the presence of $>\text{C}=\text{O}$ stretching groups (amides at $\sim 1650 \text{ cm}^{-1}$). It confirmed the presence of amino acids which may contain amide group as their side chain, i.e.

asparagine and glutamine. The spectra at $3280\text{--}3340\text{ cm}^{-1}$ showed the presence of $>\text{CH}$ -stretching vibrations. The spectra of phenylalanine, proline, valine, leucine and isoleucine were in the range of $900\text{--}3700\text{ cm}^{-1}$ (Devakate et al., 2009).

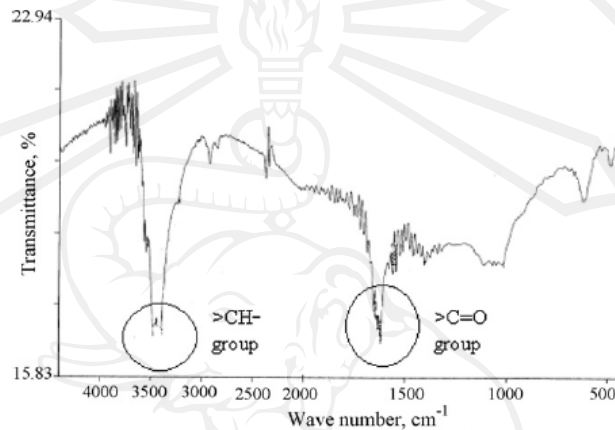


Figure 8 FTIR spectra of the freeze-dried bromelain powder (Devakate et al., 2009)

D. Differential scanning calorimetry

Differential scanning calorimetry (DSC) is an analytical technique which measures the heat flow into or out of a material as that material is exposed to a controlled thermal profile. DSC provides both qualitative and quantitative information about material transitions including glass transitions, crystallization, curing, melting and decomposition. The DSC thermogram of bromelain powder as shown in

Figure 9, the glass transition temperature was found to be $61\text{ }^{\circ}\text{C}$. The thermogram was an endotherm indicating that the powder was amorphous. It could be concluded that in order to avoid any structural changes and protein denaturation in powder the wet bulb temperature of outlet drying air should be less than $61\text{ }^{\circ}\text{C}$ (Devakate et al., 2009)

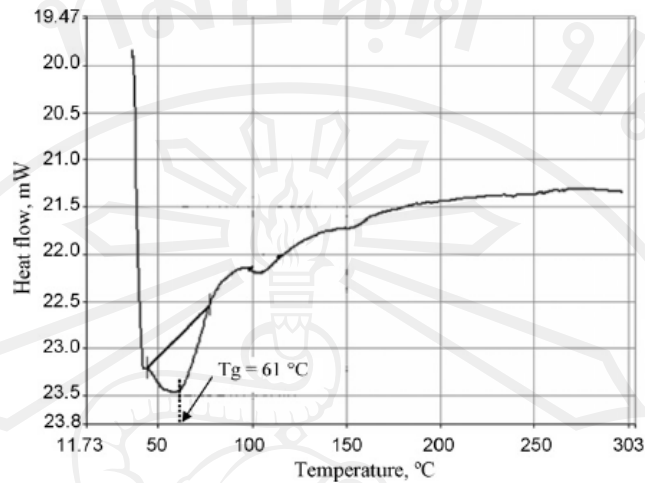


Figure 9 DSC thermogram of the bromelain powder (Devakate et al., 2009)

E. Lowry and Bradford method

Quantitative estimation of protein content are determined by Lowry and Bradford method which are the most common colorimetric assays performed by biochemists. The Lowry assay has been widely used to estimate the amount of proteins in biological samples. First, the proteins are pre-treated with copper ion in alkali solution and then the aromatic amino acids in the treated sample reduce the phosphomolybdatephosphotungstic acid present in the Folin reagent. The end product of the reaction has blue color. The concentration of protein is determined by comparing the standard curve of bovine serum albumin (BSA). The protein concentrations of the stem and fruit bromelain crude extract were 0.70 and 1.11 mg/ml, respectively which determined by Lowry's method (Gautam et al., 2010). The Bradford method is based on the absorbance shift observed in an acidic solution of dye Coomassie Brilliant Blue G-250. When added to a solution of protein, the dye binds to the protein resulting in a color

change from a reddish brown to blue. This method was used to determine the protein content of the crude extract from various parts of pineapple. The crown and leaves extract gave the highest protein content of 0.25 ± 0.01 , 0.39 ± 0.02 and 0.54 ± 0.01 mg/ml from Phulae, Nanglae and Pattawia cultivar, respectively (Sangthong et al., 2011).

1.4.4.4 Bromelain in pharmaceutical and cosmeceutical applications

A. Pharmaceutical applications

Although the exact chemical structure of all active components of bromelain is not fully determined, this substance has shown distinct pharmacological promise. Its properties include: (1) interference with growth of malignant cells; (2) inhibition of platelet aggregation; (3) fibrinolytic activity; (4) anti-inflammatory action; (5) skin debridement properties. Bromelain in doses of 10, 20 and 40 mg/kg showed 11.3, 45.1 and 56.3% inhibition of paw edema respectively at the end of 3 h, and the percentage of protection from writhing was 11.1, 23.4 and 40.8% respectively (Sudjarwo, 2005). The effect of bromelain treatment has been determined on canine articular chondrocytes *in vitro*. Chondrocytes which were exposed to 50 μ g/ml bromelain showed lower apoptotic rate and higher mitotic rate than in the control groups that were incubated with media only. Bromelain significantly decreased ($p < 0.05$) TIMP-1 and MMP-3 expression. The bromelain treatment have regarded to the healing and modulation of osteoarthritis (Siengdee et al., 2010).

B. Cosmeceutical applications

For cosmeceutical application, bromelain can help dispel blotches and pimples, clean the face and promote blood circulation making the skin

healthier and tender. Moreover, it used in face-care products to provide gentle peeling effects (Polaina and MacCabe, 2007). The previous study has been showed that the aqueous extracts from Nanglae and Phulae pineapple showed antioxidant activity. The DPPH radical scavenging activities of pineapple pulp were 152.93 ± 10.51 and 118.18 ± 8.19 $\mu\text{mol TE (Trolox equivalent)}/100\text{g FW (fresh weight)}$ for Nanglae and Phulae cultivars, respectively. The FRAP value of Nanglae cultivar was 205.73 ± 9.15 $\mu\text{mol AAE (ascorbic equivalent)}/100\text{g FW}$ which was higher in reducing power than Phulae (165.28 ± 2.04 $\mu\text{mol AAE}/100\text{g FW}$) (Kongsuwan et al., 2009).

1.4.4.5 Bromelain in scar treatment

Bromelain is a great exfoliator which can break down the connecting structure that holds surface skin cells together and remove the dead skin cells on the top layer of the epidermis or skin. It has been used successfully to debride the eschar of the scar. Bromelain was studied to used in the debridement of firearm wounds with six wound tracks in each group: wound excision (group E), wound incision (group I), bromelain (group B), incision + bromelain (group IB), and control (group C). Bromelain solution (10 mg/ml) hydrolyzed wound tissue rapidly with minimal proteolysis of normal tissue. The thickness of devitalized tissues of group IB decreased with the time of using bromelain. After topical treatment, the bacterial content was significantly less in group IB than in group I, B, and C ($p < 0.05$). The wound healing time of group IB was also shorter 14.00 ± 1.90 days (Hu et al., 2011). Debrase[®], the herbal enzymatic debriding preparation derived from bromelain (2 g bromelain in 20 g gel) was applied on burn wounds for 4 h. The total of 93% of the wounds healed by either spontaneous

epithelialisation or skin grafting and only 7% of the wounds needed additional tangential excision followed by skin grafting (Krieger et al., 2012).

1.4.5 Problems of protease enzymes in pharmaceutical and cosmeceutical applications

1.4.5.1 Chemical stability

Like many other proteins and peptides, the therapeutic uses of protease are hampered by its physico-chemical stability. Papain which is a natural protease from plants is almost unstable with its activities significant loss under high temperature (at more than 65 °C) (Afaq et al., 2001) and acidic conditions (at pH below 2.8), probably due to autolysis and oxidation. Bromelain at low concentration was more susceptible to spontaneous inactivation by water at room temperature. The diluted bromelain solution (10 mg/ml) was inactivated by low pH and the digestive enzymes such as trypsin (Hale et al., 2005).

1.4.5.2 Skin irritation

Generally, prolong skin contact with protease enzymes can cause skin irritate because these enzymes digest skin tissue which composed of proteins and peptides. The allergic reaction to skin contact with papain has also been reported (Ezeoke, 1985; Epstein, 2000). The common side effects of papain containing topical application are temporary burning sensation and mild skin irritation. Papain 0.2% (w/v) contacted to stratum corneum for 24 h could induce dramatic changes (Lopes et al., 2008), as the followings: a large amount of the intercellular materials was lost in the first

layer of stratum corneum. Then, corneosomes, identified by rudiments of their attachment plaques, were devoid of their plug material, most of extracellular components were digested and corneocytes were separated (**Figure 10**). Bromelain exhibited cytotoxicity against fibroblasts at low concentration (0.1 $\mu\text{g/ml}$) (Honda et al., 2011).

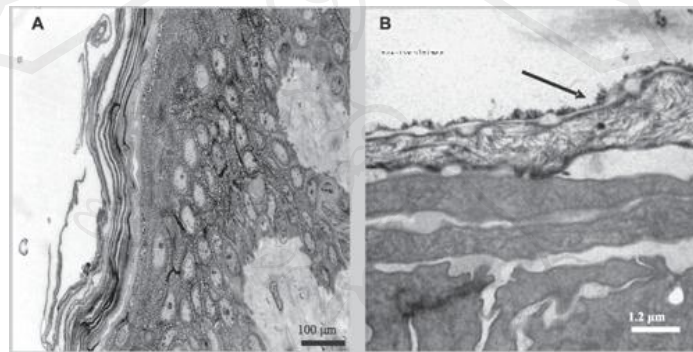


Figure 10 Micrographes from light microscope (A) and transmission electron (B) microscope of human epidermis after 24 h papain treatment indicating of the disruption of the corneosome bond (arrow) and modified the superficial stratum corneum layer (Lopes et al., 2008).

1.4.6 Transdermal delivery systems

Transdermal drug delivery systems for both local and systemic effects provide a convenient route of administration for a variety of clinical indications. However, the application of transdermal delivery is limited by the barrier function of the skin (Benson, 2005). In order to overcome this problem and optimize the transdermal delivery systems, it is necessary to understand the structure of the skin and pathways of skin penetration.

1.4.6.1 Skin structure and routes of skin penetration

The skin consists of three layers including the epidermis, dermis and hypodermis (**Figure 11**). The epidermis thickness ranges between 50 to 100 μm . It is composed of a dead layer of cells called “stratum corneum” (10 to 20 μm thick on most of the body surface). These cells are flat and mainly composed of keratin, a quite rigid and hard material. The stratum corneum forms a protective shield for covering the underlying viable epidermis composed primarily of keratinizing epithelial cells. This horny layer is the result of the two biological processes which are differentiation and proliferation of keratinocytes that compose the living epidermis. The dermis, depending on the anatomical sites, is mainly composed of collagen and elastin fibers embedded in a viscous medium made of water and glycoproteins. Fibers of the upper dermis (or papillary dermis) are thinner than those present in the deep dermis. The total thickness varies according to the site from 1-3 mm. Hypodermis is quite variable in thickness depending on persons, and the position on the body. It is mainly composed of cells (adipocytes).

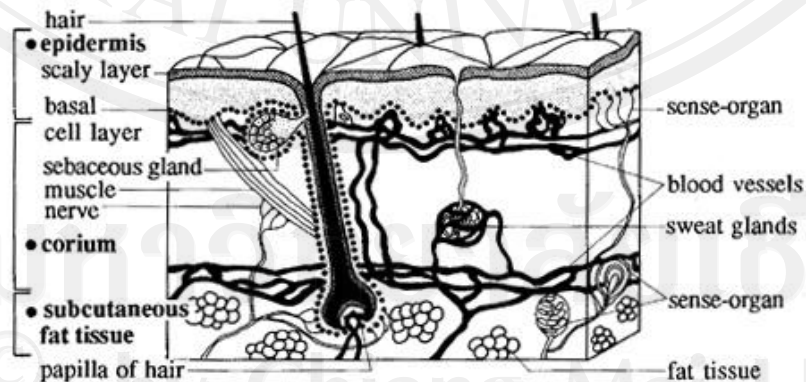


Figure 11 Skin structure of human skin (Umbach, 1991)

Currently, only a small number of transdermally delivered drugs are commercially available despite the potential advantages of this route. Ideal characteristics for successful transdermal delivery are a relatively low molecular weight (<500 Da) and melting point (<200 °C), moderate lipophilicity (log P 1-3) and aqueous solubility (>1 mg/ml) and high pharmacological potency (Benson et al., 2008). The drug applied to the skin surface has three potential pathways across the epidermis including skin appendages such as hair follicles, sweat ducts and sebaceous glands (shunt routes), through the corneocytes and the lipid lamellae (transcellular route), or along the tortuous pathway along the lipid lamellae (intercellular route) (**Figure. 12**). A particular drug is likely to permeate by a combination of these routes, with the relative contributions of these pathways to the gross flux governed by the physicochemical properties of the molecule.

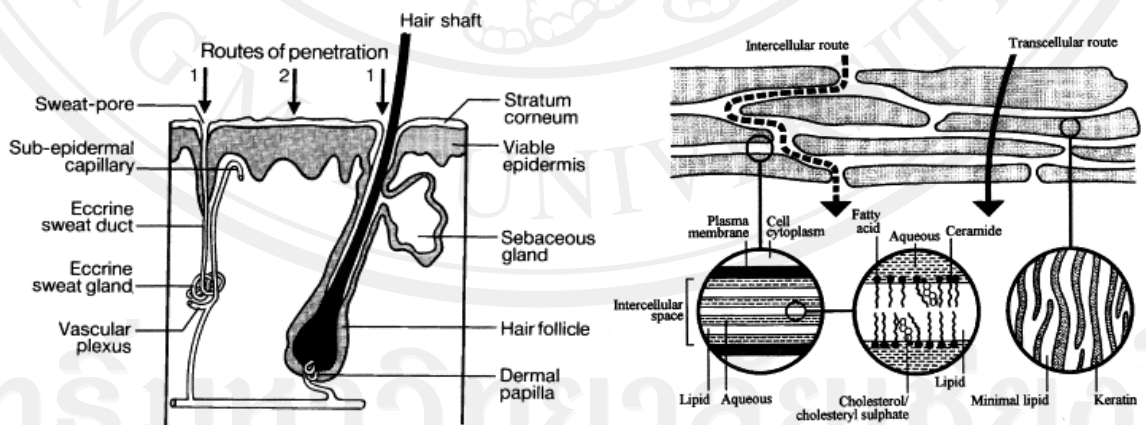


Figure 12 Three main pathways of skin penetration including transappendageal, intercellular and transcellular pathway (Barry, 2001)

1.4.6.2 Advantages of transdermal delivery systems

The skin covers the total surface area of approximately 1.8 m² and provides the contact between the human body and the external environments. Dermal drug delivery is the topical application of drugs to the skin for the treatment of many skin diseases. The therapeutic benefits of transdermal delivery systems are the sustained delivery of the drugs (to provide a steady plasma profile, particularly for drugs with short half-lives, and hence reduced the systemic side effects). This delivery system will reduce the typical dosing schedule to once daily or even once weekly, hence generating the potential for the improved patient compliance and the avoidance of the first-pass metabolism effect for drugs with poor oral bioavailability. Additionally, transdermal delivery represents a convenient, patient-friendly option for drug delivery with the potential for flexibility, easily allowing dose changes according to patient needs and the capacity for self-regulation of dosing by the patients. Alternatively, transdermal delivery can be used in the situations requiring the minimal patient cooperation, for examples, in situations involving administration of drugs by someone other than the patients. The non-invasive character of transdermal delivery makes it accessible to a wide range of patient populations and a highly acceptable option for drug dosing. Nowadays, eight drugs based on transdermal delivery system are currently in the market including clonidine, estradiol, nitroglycerine, fentanyl, testosterone, scopolamine, nicotine, oxybutinin, and recently methylphenidate, selegiline, rivastigmine and rotigotine (Farahmand et al., 2009).

1.4.6.3 Skin penetration enhancement of peptides

Peptides are hydrophilic and often charged molecules at the physiological pH. Their molecular weights are from 300 Da to greater than 1000 kDa. Consequently, their skin permeation is poor and despite generally having high potency, they are ineffective if administered transdermally. Several penetration enhancement techniques have been developed to overcome the skin barrier and facilitate the permeation of peptides and proteins through the skin. These strategies include chemical modification to form a conjugate with an increased lipophilicity and encapsulation into the hydrophobic carriers, application with the penetration enhancers which chemically or physically reduce the stratum corneum barrier (**Figure. 13**). Examples of the successful enhancement approaches are summarised in **Table 5**.

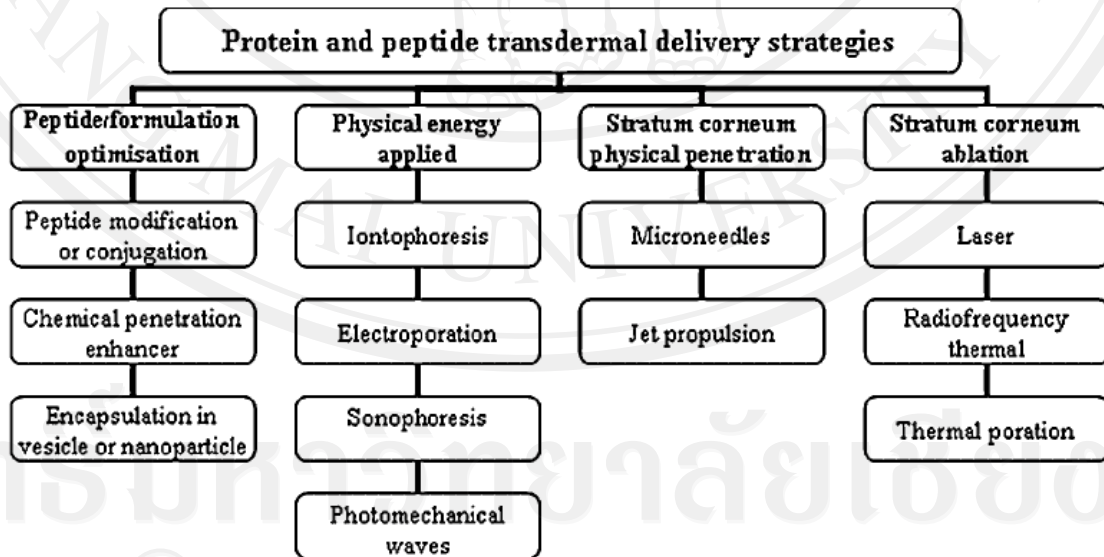


Figure 13 Strategies for optimisation of protein and peptide drug permeation across the skin (Benson and Namjoshi, 2008)

Table 5 Examples of the delivery methods to enhance protein/peptide across the skin (Benson and Namjoshi, 2008)

Protein/Peptide	Delivery method	Outcome
TRH	Chemical: terpene and ethanol	Five folds increase in flux to 1.6 mg/cm ² h <i>in vitro</i> in human epidermis
IFN- α	Liposome	Increased skin deposition
IFN- α	Chemical modification to increase lipophilicity	5-6 times increase in skin penetration <i>in vitro</i> in human skin
LHRH	Chemical enhancer combinations	Up to 100-fold increase in skin permeability
LHRH	Iontophoresis	Flux up to 9.87 mg/cm ² h in cadaver skin
LHRH	Iontophoresis and limonene	10-fold increase in skin permeability
Nafarelin	Iontophoresis	Flux up to 6.47 mg/cm ² h in cadaver skin
Calcitonin	Iontophoresis	Steady state blood concentration 7.6 ng/ml in hairless rats: comparable to sc injection
Heparin	Chemical enhancer combinations	Up to 100-fold increase in skin permeability
Heparin	Electroporation	100–500 mg/cm ² h <i>in vitro</i> in human skin
Heparin	Electroporation and anionic phospholipid	20-folds increase in insulin transport compared to electroporation alone
Insulin	Sonophoresis	Insulin levels sufficient to reduce blood glucose in pigs
Insulin	Photomechanical waves	Insulin levels sufficient to reduce blood glucose in diabetic rats
Insulin	Microneedles	Insulin levels sufficient to reduce blood glucose in diabetic rats
Insulin	Peptide transporter	Insulin levels sufficient to reduce blood glucose in rats
Insulin	Electroporation and iontophoresis	Insulin levels sufficient to reduce blood glucose in rats
Desmopressin	Microneedles	Pharmacologically relevant blood levels in hairless guinea pig within 5-15 min
Vaccine examples		
Recombinant H5 hemagglutinin	Thermal ablation (PassPort)	Stimulation of immune system against avian H5N1 influenza virus in mice
Hepatitis B surface antigen	Elastic liposomes	Systemic and mucosal antibody response elicited in mice
Hepatitis B virus DNA vaccine	Jet propulsion (Powderject)	Application to healthy human volunteers resulted in both humoral and cell-mediated immune responses

1.4.6.4 *In vitro* skin transdermal absorption by Franz diffusion cells

A well-known technique for *in vitro* permeation investigation is by using the Franz diffusion cell apparatus (**Figure 14**). The technique utilizes a sampling cell which contains a solution reservoir and a sampling port, the top portion of the Franz cell is covered with the biologic membrane or skin substitute. The formulation is added to the top of the cell and periodic samples are taken from the cell reservoir and assays are piloted versus time to develop a time-penetration profile. The permeation parameters such as cumulative amount, steady-state flux (J_{ss}) or lag time (t_L) were determined (Rhee et al., 1999). The penetration profiles were constructed by plotting the total amount of drug penetrated versus time. The x -intercept of the extrapolated linear region of the curve gave t_L . The slope of the linear portion of the profile, determined by linear regression analysis, was J_{ss} .

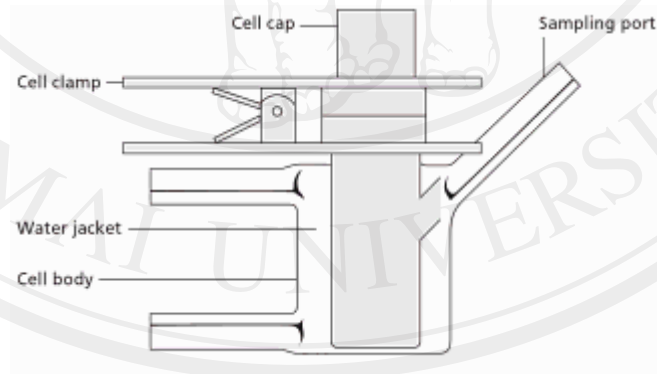


Figure 14 The Franz diffusion cell apparatus (Cornell et al., 2010)

The previous study has examined the rate and extent of transdermal penetration of three synthetic hexapeptides consisting of only glycine (Gly) and phenylalanine (Phe) as the constituent amino acids through rat skin by vertical Franz diffusion cells. The

effect of various vehicles (additionally some terpenes including carveol, cineole and menthone, along with ethanol) to enhance the transdermal permeation were determined. The peptides were more rapidly penetrated through the skin in the presence of terpene. Among the terpenes tested, cineole was the most effective for all three peptides (Ham et al., 2007). It has investigated transdermal absorption of gallidermin (Gdm) loaded in niosomes through rat skin by vertical Franz diffusion cells (Manosroi et al., 2010b). Gdm loaded in niosomes and incorporated in gel exhibited the highest cumulative amounts ($82.42 \pm 9.28 \mu\text{g}/\text{cm}^2$) and fluxes ($13.74 \pm 1.55 \mu\text{g}/\text{cm}^2/\text{h}$) in stratum corneum (SC). But, Gdm loaded in this formulation gave the comparative cumulative amounts ($183.16 \pm 30.32 \mu\text{g}/\text{cm}^2$) and fluxes ($25.74 \pm 5.05 \mu\text{g}/\text{cm}^2/\text{h}$) in VED (viable epidermis and dermis) to the unloaded Gdm incorporated in gel (**Figure 15**).

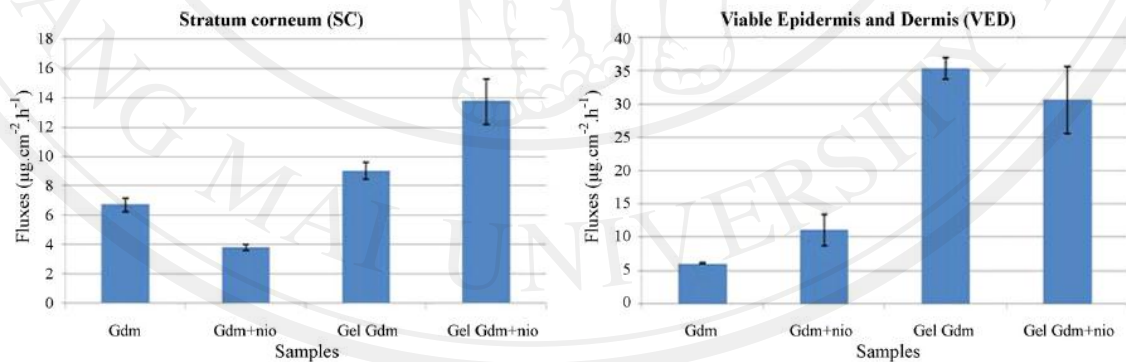


Figure 15 The fluxes ($\mu\text{g}/\text{cm}^2/\text{h}$) of Gdm from various systems in stratum corneum (SC) and viable epidermis and dermis (VED), at 6 h by vertical Franz diffusion cells. Gdm: Gdm in phosphate buffer (20 mM, pH 5.4); Gdm+nio: Gdm loaded in niosomes; Gel Gdm: Gdm incorporated in gel; Gel Gdm+nio: Gdm loaded in niosomes and incorporated in gel.

1.4.7 Nanocarrier delivery systems

As known, protease enzymes also have low chemical stability, skin irritation and low percutaneous penetration. For keloids and hypertrophic scars application, the major barrier of skin penetration is the excessive accumulation of collagen of the scars. Novel technologies such as nanocarrier systems have been used to stabilize, enhance percutaneous absorption, increase safety and efficacy of these enzymes. Generally, nanocarrier systems are classified as nanovesicular and nanoparticulate delivery systems (Castro et al., 2008).

1.4.7.1 Nanovesicles

Nanovesicles have hydrophilic as well as lipophilic features. They can entrap both water-soluble and oil-soluble substances. The hydrophilic substances can be entrapped in their inner compartment and lipophilic substances can be inserted in their bilayer membrane.

A. Classification of nanovesicles

Nanovesicles including niosomes and liposomes, have recently attracted attention from their competency to improve transdermal penetration. In general, vesicles made of natural or synthetic phospholipids are called liposomes, whereas those made of nonionic surfactants (e.g. alkyl ethers and alkyl esters) are called niosomes.

Liposomes: They are the most widely known nanovesicular delivery systems.

Liposomes are unilamellar or multilamellar spheroid structures composed of lipid molecules, often phospholipids, assembled into bilayers. It has been used for delivery of

interferon α -2b (IFN α -2b), which are cytokines with anti-proliferative activities. IFN α -2b could be used to treat dermal fibroproliferative disorder such as keloid and hypertrophic scar. However, there are many practical drawbacks to the systemic or intralesional administration. Normally, topical administration of IFN α -2b in solution is not effective because the free cytokine does not penetrate the epidermis efficiently. IFN α -2b could be encapsulated in liposomes without losing its anti-fibrogenic effects on dermal fibroblasts in culture (Ghahary et al., 1997). Moreover, cream containing liposome-encapsulated IFN α -2b was more effective than liposome alone in reducing the scar formation in a rabbit fibrotic ear model (Lee et al., 2005b). Recently, it has been reported that when papain loaded in liposomes, papain could effectively pass through the skin (Roslan et al., 2010). However, liposomes have problems of variable purity, high cost of phospholipids and limited shelf life due to the rancidification of the lipid compositions.

Niosomes: They have been studied as an alternative to liposomes in order to overcome the problems associated with sterilization, large-scale production and stability. Niosomes are formed from non-ionic surfactants in aqueous media resulting in closed bilayer structures. In recent years, niosomes have been extensively studied for their potential to serve as a carrier for the delivery of drugs, antigens, hormones and other bioactive agents (Arora et al., 2007). *In vitro* study conducted by Yoshida et al, the oral delivery of a vasopressin derivative entrapped in niosomes showed that entrapment of the peptide drug was significantly more chemical stability than the free drug (Yoshioka et al., 1992). Human insulin (100 IU/kg) loaded in niosomes composed of polyoxyethylene

alkyl ether surfactants (Brij 52 and Brij 92) or sorbitan monostearate (Span 60) and cholesterol showed decreased levels of blood glucose and elevated serum insulin. The insulin loaded in Brij 92 niosomes exhibited the highest hypoglycemic effect (Pardakhty et al., 2011). Recently, niosomes has not been studied for the entrapment of papain and bromelain.

B. Methods of preparation

Various types of nanovesicles can be prepared by very different methods implying that there are several mechanisms operating in the nanovesicular formulations. **Table 6** showed the preparation methods of nanovesicles. The effect of preparation technique on the properties of liposomes encapsulating ketoprofen-cyclodextrin complexes was investigated. Liposomes were prepared with different techniques, such as thin layer evaporation, freezing and thawing, extrusion through microporous membrane, and reverse phase evaporation method, obtaining multi-lamellar vesicles (MLV), frozen and thawed MLV (FATMLV), small uni-lamellar vesicles (SUV) and large unilamellar vesicles (LUV), respectively. Encapsulation efficiency was in the order of $MLV > LUV > SUV$, whereas the drug permeation rate was in the order $SUV > MLV = FATMLV > LUV$ (Maestrelli et al., 2006). Niosomes can be prepared by the similar method to liposomes.

C. Physical characteristics of nanovesicles

Physical characterization of nanovesicles investigations which are frequently used in drug delivery system development and found in several studies are following:

Table 6 Preparation methods of nanovesicles (Uhumwangho et al., 2005)

Methods	Principles	Types of nanovesicles
Hand-shaken methods (Thin-film method)	Thin lipid film is deposited on the walls of a round-bottomed flask and shaken in excess of aqueous phase.	MLV
Sonication method	There are two techniques: either the tip of sonicator is immersed into nanovesicular dispersion or a sample in a tube or beaker is placed into a bath sonicator.	SUV
High-pressure extrusion method	The reducing of the nanovesicular sizes by the extrusion through the capillary or the polycarbonate membrane (0.8-1.0 μm) under high pressure (up to 250 psi).	SUV
Ether injection method	The solution containing composition of nanovesicles in ether is slowly injected into the preheated aqueous solution of the drugs maintained at 60°C through the specified gauze needle.	UV
Solubilisation and detergent removal method	It involves the use of detergent (surfactant) for the solubilisation of the lipids. The detergent is subsequently removed by dialysis or column chromatography.	LUV
Reverse phase evaporation technique	It consists of a rapid injection of aqueous solution of the drug into an organic solvent, which contains the lipid dissolved with simultaneous bath sonication of the mixture.	LUV
Freeze-dried rehydration method	The freeze dried powder can be reconstituted to an aqueous suspension immediately before use.	MLV
Microfluidization method	It is based on submerged jet principle in which two fluidized streams interact at ultra high velocities, in precisely defined micro channels within the interaction chamber.	UV
Supercritical carbon dioxide fluid technique (scCO ₂)	Supercritical carbon dioxide (scCO ₂) has been used for the substitution of organic solvent to prepare bilayer vesicular formulations with the advantages of not only being environmental friendly, non-toxic and nonflammable.	MLV

Note: MLV: multilamellar vesicles, SUV: small unilamellar vesicles, UV: unilamellar vesicles and LUV: large unilamellar vesicles

Vesicular sizes: The particle size is an important parameter in in-process control and particularly in quality assurance, because the physical stability of vesicle dispersions depends on particle size and particle size distribution. Dynamic light scattering (DLS) is a relatively fast method of characterizing the size of molecules in solution. DLS detects the fluctuations of the scattering intensity due to the Brownian motion of molecules in solution. Dynamic light scattering measurements are made on the fixed scattering angle Zetasizer Nano system (Malvern Instruments Ltd., Malvern, UK). Samples are measured in a quartz cuvette. The resulting data are analysed by the DTS software (Nobbmann et al., 2007). In fact, the small size of the niosomes can increase the physical stability of the formulation according to the Stokes' law indicating that the velocity of a droplet is proportional to the square of its radius (Fustier et al., 2010). DLS software can analyze the size distribution in the term of polydispersity index (PDI). The maximum value of PDI is limited to 1.0. The PDI value of 1 indicates that the sample has a very broad size distribution and may contain large particles or aggregates.

Zeta potential values: The zeta potential of the nanovesicular formulation depends on the movement of the vesicles (electrophoretic velocities). Zeta potential is measured by applying an electric field across the dispersion. The charge particles within the dispersion migrate toward the electrode of opposite charge with a velocity proportional to the magnitude of the zeta potential. Samples are measured in the disposable capillary cell which is the only cell with entirely disposable cuvette and electrodes. If the zeta potential is reduced below a certain value (inside the ± 30 mV range), the attractive forces between the vesicles due to van der Waals' force, overcome

the forces of the repulsion and the particles come together to form aggregation (Nutan et al., 2009). The suitable range for the stable nanovesicular formulation should be outside the ± 30 mV range (Gibson et al., 2009).

Morphology of nanovesicles: The nanostructure of nanovesicular systems can be visualized with the high-magnification power of the electron microscope. Transmission electron microscopy (TEM) is a powerful tool for the investigation of the microstructure of materials, providing crystallographic information and composition at the nanometer scale. TEM specimen preparation involves the thinning of the specimens to the electron transparent thickness. The morphology of nanovesicles is performed on small copper discs called grids cast with a fine mesh. After a small drop of the sample is placed on the hydrophilic grid, it needs to be stained so that the sample can be easily differentiated from the background. However, aqueous samples do not survive the high vacuum of an electron microscope and water loss occurs leading to microstructure changes. Therefore, special techniques of sample preparation are necessary prior to electron microscopy. Freeze fracture has proven to be successful at overcoming these problems (Müller-Goymann, 2004).

Entrapment efficiency: This characteristic is the amount of the drug loaded inside the nanovesicles and can be obtained from the total amount of loaded drug divided by the total initial input of drug. To calculate the entrapment efficiency of nanovesicular formulation, it needs to separate the free drug from the encapsulated drug using various separation techniques such as centrifugation, size exclusion chromatography and dialysis. The ultracentrifugation method is the most widely used technique for determining the

entrapment efficiency because it is the fastest and simple to use. The nanovesicular dispersion is centrifuged and then the clear supernatants are removed carefully to separate free drug. Size exclusion chromatography, also called gel filtration is a separation technique used to separate molecules on the basis of size and shape. The gel filtration matrices such as Sephadex[®], Sephacryl[®] and Sepharose[®] contain pores with tunnels in which the size can be controlled depending on the size of molecules to be separated. Small molecules can penetrate the pores and enter the beads. However, larger molecules do not enter the beads and are excluded first from the column. Therefore, the drug loaded in nanovesicles which larger molecules elute before the free drug that is the smaller molecules (Hou et al., 2007). Recently, the microdialysis (MD) technique has also been used to determine the entrapment efficiency of nanovesicles. The free drug would diffuse into the probe because there is a concentration gradient of the free drug from the outside to the inside of the MD fiber. The molecular weight cutoff of the MD membrane such as nanostructures and the incorporated drug can not cross the membrane (Yue et al., 2009). After separation, the vesicular structure was ruptured by adding Triton X-100 or alcohol before the drug amount analysis.

D. Elastic nanovesicles

Conventional nanovesicles are usually not efficient to transdermally deliver across the skin, because they do not deeply penetrate the skin. But, they rather remain on the upper layer of stratum corneum (SC). Several researchers have developed novel elastic nanovesicles in order to deeply and easily penetrate through the skin. These vesicles can better facilitate drug transport across the skin as compared to

conventional vesicles since they can squeeze through small pores in SC which are smaller than their vesicular sizes. The examples of elastic nanovesicles are transfersomes (vesicles containing phospholipid and edge activator), bilosomes (vesicles containing bile salt) and ethosomes (vesicles containing penetration enhancers such as alcohols and polyols). Ethanol is known as an efficient permeation enhancer which has been widely used in elastic vesicular formulation. It can interact with the polar head group region of the lipid molecules, resulting in the reduction of the melting point of the SC lipid, thereby increasing lipid fluidity, and cell membrane permeability (**Figure 16**).

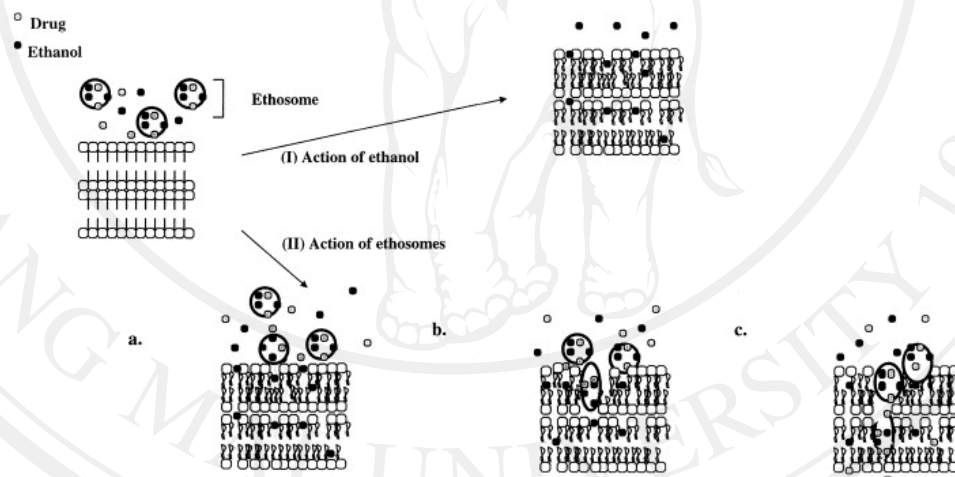
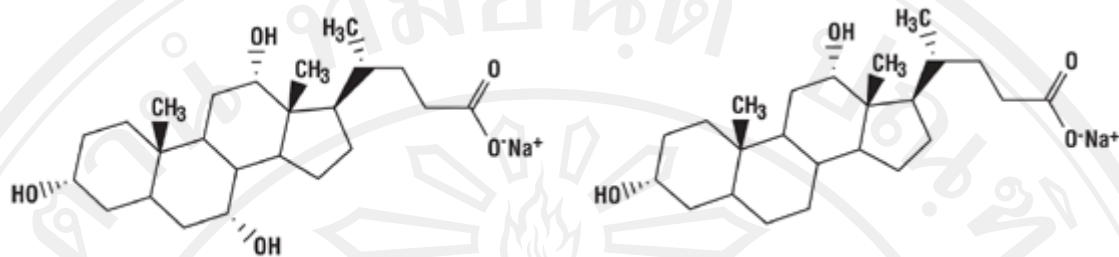


Figure 16 Mechanism to penetrate the skin of ethosomes (Touitou et al., 2000)

However, because of the interdigitation effect of ethanol on the lipid bilayers, vesicles can not coexist with high concentrations of ethanol. Also, high content of ethanol could affect the membrane structure and increase the cytotoxicity. Several literatures have reported that ethanol is toxic to human dermal fibroblast cells. It has

been reported that ethanol was mild-moderate toxic on human three-dimensional physiologic skin model (Triglia et al., 1991). Ethanol was toxic to human skin cells in both a dose- and time-dependent manner. The mechanism by which this damage occurs was a complex process that probably involved alternation of cytokine (TNF- α), and changed in the apoptotic activity and structure of skin cells (Neuman et al., 2002). Recently, edge activators have been used to prepare elastic vesicles instead of ethanol (Lee et al., 2005a).

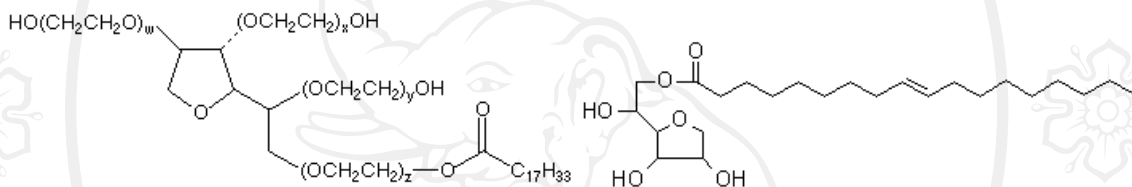
Edge activators used in elastic nanovesicles: An edge activator is often a single chain surfactant that destabilizes the lipid bilayer of the vesicles and increases the deformability of the bilayer by lowering its interfacial tension. The widely used edge activators including sodium cholate (NaC), sodium deoxycholate (NaDC), Tween 80 and Span 80 have been introduced to develop the less cytotoxic elastic nanovesicles. The chemical structures of edge activators are shown in **Figure 17**. These edge activators may decrease the transition temperature (T_m) of the vesicles and induce the phase transition of the vesicles to liquid crystalline phase resulting in the increase of vesicle elasticity (Manosroi et al., 2011c). The edge activators were affected to nanovesicular characteristics such as vesicular sizes, zeta potential values and entrapment efficiency (EE). Transfersomes prepared with 95:5% (w/w) (phosphatidylcholine:edge activator) ratio showed %EE in order of Span 85>Span 80>NaC>NaDC>Tween 80 (El Zaafarany et al., 2010).

**Sodium cholate (NaC)**

(<http://www.piercenet.com/media/SodiumCholate.gif>)

Sodium deoxycholate (NaDC)

(<http://www.piercenet.com/media/SodiumDeoxycholate.gif>)

**Polysorbate 80 (Tween 80)**

(http://www.wcaslab.com/gif/Tween80_molecule.gif)

Sorbitan oleate 80 (Span 80)

(<http://discovery.kcpc.usyd.edu.au/9.5.5/images/span80.gif>)

Figure 17 Chemical structures of sodium cholate (NaC), sodium deoxycholate (NaDC), Tween 80 and Span 80

Measurement of deformability index (DI): Elasticity of the vesicular membrane is an important and unique parameter of the deformable vesicles. The elasticity property has been investigated using various techniques. Spin label techniques have been widely used to investigate lipid mobility in biological membranes and vesicles. Using spin label techniques, information can be obtained about the influence of for example hydration state, lamellarity, curvature and physical state of vesicles. Electron spin resonance (ESR) was used to gain information on the fluidity of the vesicle bilayers using the spin labels 5-, 12-, and 16-doxyl stearic acid (5-, 12-, and 16-DSA). ESR spectra are determined with spectrometer. Typical parameters by which vesicle bilayer

dynamics and ordering are characterized the order parameter S and the rotational correlation time τ_0 . The order parameter S is the measure of the average angular deviation of the fatty acid acyl chain of the spin label probe at the nitroxide group from the average orientation of the fatty acids in the membrane. The S value of 1.0 is characteristic for a rigid lipid environment and a reduction in this value means an increase in the fluidity of the membranes. The extrusion rate of vesicles was measured to estimate values of elasticity. The elasticity of bilayers is directly proportional to $j(r_v/r_p)^2$. j was the rate of penetration through a permeability barrier, r_v was the size of vesicles and r_p was the pore size of the barrier. To measure j the vesicles were extruded through polycarbonate filters with a small pore size of nanoscale (r_p). The amount of suspension, which was extruded during 10 min, was weighed (j). In addition, transmission and scanning electron microscopy studies were carried out to examine the penetration of vesicle suspensions into filters, which is in fact also a measure for the elasticity of the vesicles (Bergh et al., 2001).

E. Application of elastic nanovesicles in topical pharmaceuticals and cosmeceuticals

The use of elastic nanovesicles as a vesicular drug carrier could overcome the limitation of low penetration ability of conventional nanovesicles across the skin. Several elastic nanovesicles for topical pharmaceuticals and cosmeceuticals had been reported. **Table 7** summarizes the application of elastic nanovesicles for transdermal drug delivery through animal and human skin (Choi et al., 2005). The advantages of nanovesicles are not only to increase the stability of the

chemicals and decrease of the skin irritation for those irritating substances, but also to enhance the transdermal permeation. Both non-elastic and elastic niosomes showed decreasing irritation of gallic acid in rabbit skin because of the reduction of the direct contact between gallic acid and the skin (Manosroi et al., 2011b). Gallarate et al. have formulated several deformable liposomes by using hydrogenated soya lecithin (HPC) and

Table 7 The application of elastic nanovesicles for transdermal drug delivery through animal and human skin (Choi and Maibach, 2005)

Drugs	Animal	Composition	Enhancing factor
Dipotassium glycyrrhizinate (KG)	Pig	PC:KG (4:1)	5.9
		HPC:KG (4:1)	5.5
Methotrexate	Pig	PC:KG (2:1)	5.2
		HPC:KG (2:1)	5.9
Dexamethasone	Rat	PC:cholesterol (7:3)	1
		PC:deoxycholate (85:15)	2.2
		PC:Tween-80 (85:15)	1.9
		PC:Span-80 (85:15)	2.3
Diclofenac	Rat	Commercial form	1
		Lotion-like transfersomes	30-100
Gap junction protein (antibody production)	Mouse	Soybean PC	1
		PC/sodium cholate/SDS	4.7
Insulin	Mouse	PC liposomes or micelle	No change
		PC/cholate (8.7:1.3)	20-30%
Cyclosporin A	Mouse	PC/cholate (10:2.8)	16.2
Oestradiol	Human	PC/cholate (84:16)	18
		PC/Span 80 (84:16)	16
		PC/Tween 80 (84:16)	15
		PC/oleic acid (84:16)	13
5-Fluorouracil	Human	PC/cholate (84:16)	6.9-13.2
Rotigotine	Human	L-595/PEG-8-L (50:50)	30.6
Pergolide	Human	L-595/PEG-8-L (50:50)	2.7

Note : PC= phosphatidylcholine, HPC= hydrogenated phosphatidylcholine, SDS= sodium dodecyl sulfate, L-595= sucrose laurate ester and PEG-8-L= octaoxyethylene laurate ester

different edge activators including sodium cholate (SC), polysorbate 80 (T80), dipotassium glycyrrhizinate (DPG) and saccharose monopalmitate (SMP). The deformable liposomes obtained were able to entrap α -tocopherol and tocopheryl acetate up to 0.17% (w/w). When α -tocopherol was introduced in undeformable liposomes, the residual amount within the skin was far lower than that obtained with deformable liposomes. In fact, α -tocopherol skin deposition from deformable liposomes was almost four times more than that from undeformable ones (Gallarate et al., 2006).

For hypertrophic scar treatment, the previous study has compared the scar penetration efficiency and retention between ethosomes (ES) and deformable liposomes (DS) both encapsulated with 5-fluorouracil (5-FU). ES had better permeability of 5-FU than DS of 1.16 times, DS had higher entrapment efficiency of 5-FU, and more 5-FU deposition in hypertrophic scar than ES (Wo et al., 2011). The permeation profiles of 5-FU loaded in ES exhibited no lag times, showing a significant amount of 5-FU after 1 h. The accumulation of 5-FU in hypertrophic scar (HS) after 24 h ($24.52 \pm 2.32\%$ of the applied dose) was significantly ($P < 0.001$) higher than in skin ($1.47 \pm 0.48\%$ of the applied dose). The 30% hydroethanolic solution in both HS and skin showed a permeation profile characterized by a lag time of 3 h. However, the total amount of 5-FU that permeated HS after 24 h ($8.19 \pm 4.37\%$ of the applied dose) was significantly ($P < 0.01$) greater than the amount observed in skin ($0.45 \pm 0.17\%$ of the applied dose) (Zhang et al., 2012). However, the entrapment of papain and bromelain in elastic niosomes composed of edge activators has not been studied.

1.4.7.2 Nanoparticles

Nanoparticles are in the solid state, and either amorphous or crystalline. They are able to adsorb and/or encapsulate a drug, thus protecting it against chemical and enzymatic degradation. Nanoparticles as drug carriers can be formed from different materials. In addition to solid lipids, both biodegradable polymers and nonbiodegradable polymers have been used as carrier materials.

A. Classification of nanoparticles

Nanoparticles are divided into two categories including nanocapsules and nanospheres. Nanocapsules are reservoir form, which have the substance is confined to a cavity consisting of an inner liquid core surrounded by a polymeric membrane. Nanospheres are matrix type of structure. The substance may be absorbed at the sphere surface or encapsulated within the particle. Considering the encapsulation mechanisms, the substance can be entrapped, dispersed, dissolved within or adsorbed on the nanoparticles (**Figure 18**).

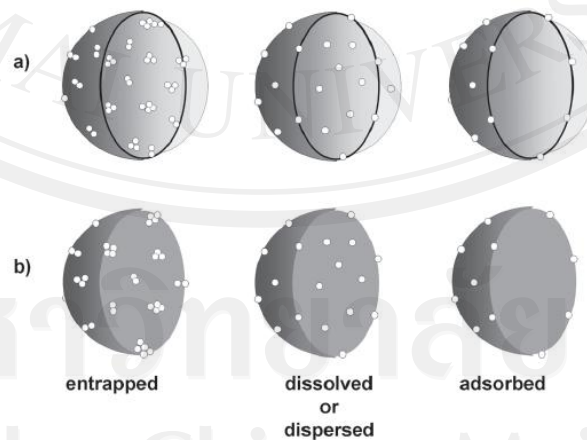


Figure 18 Encapsulation mechanism models: drug entrapped in, dissolved or dispersed within, and adsorbed on: a) nanocapsules and b) nanospheres (Guterres et al., 2007).

B. Methods of preparation

The preparation methods of nanoparticles can be classified into two main categories according to whether the formulation requires a polymerization reaction or is achieved directly from a macromolecule or polymer. Many methods for the preparation of nanoparticles include two main steps. The preparation of an emulsified system corresponds to the first step while the nanoparticles are formed during the second step of the process. This second step is achieved either by the precipitation or the gelation of a polymer or by polymerization of monomers. A few other methods do not require the preparation of an emulsion prior to the obtaining of the nanoparticles. They are based on the precipitation of a polymer in conditions of spontaneous dispersion formation or thanks to the self assembly of macromolecules to form nanogels or polyelectrolyte complexes from a polymer solution. The most important methods for the preparation of nanoparticle, together with their advantages and disadvantages are summarized in **Table 8**. The commonly utilized techniques for loading hydrophilic molecules in PLGA nanospheres are the emulsion solvent diffusion (ESD) and the emulsion solvent evaporation (ESE) techniques.

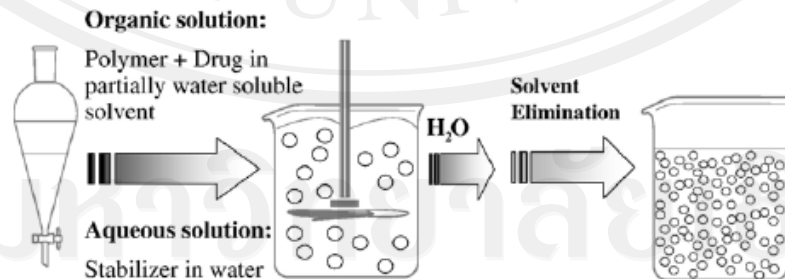
Emulsion solvent diffusion method: This method is based on the use of organic solvents, and then it is adapted to the following salting-out procedure. The procedure is shown in **Figure 19**. In the process, nanoparticles are formed via transient emulsion droplets of drug and polymer produced by the interaction between drug and water-miscible solvent. The solvent is extracted by diffusion into the water phase, depositing the drug and polymer in the droplet. ESD method has several advantages,

Table 8 The advantages and drawbacks of the preparation methods (Reis et al., 2006)

Method	Simplicity of procedure	Need for purification	Facility scaling-up	Encapsulation efficiency (%)	Safety of compounds
<u>Polymerization of monomers</u>					
Emulsion polymerization					
- Organic	Low	High	NR	Low	Low
- Aqueous	High	High	High	High	Medium
Interfacial polymerization	Low	High	Medium	High	Low
<u>Preformed polymers</u>					
Emulsification/solvent evaporation	High	Low	Low	Medium	Medium
Solvent displacement and interfacial deposition	High	NR	NR	High	Low
Salting out	High	High	High	High	Low
Emulsion/solvent diffusion	Medium	Medium	High	High	Medium

Note: NR=no reference available.

such as simplicity, no need for homogenization, high batch-to-batch reproducibility and ease of scaling up. However, this method also has some disadvantages of high volumes of water to be eliminated from the suspension, and the leakage of water-soluble substance into external phase during emulsification resulting in the reduction of encapsulation efficiency (Reis et al., 2006).

**Figure 19** Procedure of emulsion solvent diffusion (ESD) method (Reis et al., 2006)

Emulsion solvent evaporation method: The ESE method can improve the formulation characteristics including small size, low size distribution and high encapsulation efficiency (Cohen-Sela et al., 2009). The first step requires emulsification of the polymer solution into an aqueous phase (**Figure 20**). During the second step, the polymer solvent is evaporated inducing polymer precipitation as nanoparticles.

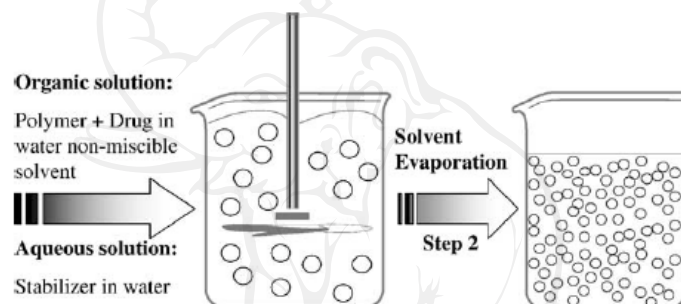


Figure 20 Procedure of emulsion solvent evaporation (ESE) method (Reis et al., 2006)

C. PLGA nanospheres

The polymer matrix that mainly used to formulate nanospheres is polylactic polyglycolic acid co-polymer (PLGA), a FDA approved biodegradable and biocompatible polymer. PLGA prepared from L-poly lactide (L-PLA) and poly glycolide (PGA) are crystalline co-polymers while those from D,L-PLA and PGA are amorphous in nature (**Figure 21**). It has been found that PLGAs containing more than 70% glycolide are amorphous in nature. The degree of crystallinity and the melting point of the polymers are directly related to the molecular weight of the polymer. The mechanical strength, swelling behavior, capacity to undergo hydrolysis and,

subsequently, the biodegradation rate are directly influenced by the crystallinity of the PLGA polymer. The resultant crystallinity of the PLGA co-polymer is dependent on the type and the molar ratio of the individual monomer components (lactide and glycolide) in the copolymer chain. PLGA polymers containing 50:50 ratio of lactic and glycolic acids are hydrolyzed much faster than those containing the higher proportion of either of the two monomers. The homopolymers of lactic acid (polylactide) and glycolic acid (polyglycolide) show poor solubilities. PLGA can be dissolved by a wide range of common solvents, including chlorinated solvents, tetrahydrofuran, acetone or ethyl acetate.

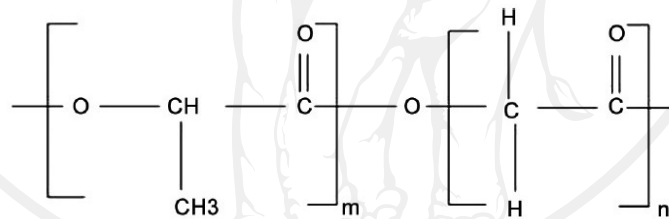


Figure 21 Chemical structure of polylactic polyglycolic acid co-polymer (Muthu, 2009)

The PLGA nanoparticles are safe for human application because of their biodegradability, increase the shelf-life, protect from degradation and control the release over a longer period of time of the entrapped substances (Vilaa et al., 2002; Rahimnejad et al., 2009). Nanospheres using PLGA polymers are commonly formulated by an emulsion-solvent evaporation technique. PLGA nanospheres have been reported to be effective as delivery systems for several peptides such as cyclosporine A (Malaekhe-Nikouei et al., 2005), insulin (Cui et al., 2006; Liu et al., 2007b) and salmon calcitonin

(Jang et al., 2007). The particular sizes and zeta potential values of PLGA nanospheres was determined by a laser particle size analyzer, based on a dynamic light scattering concept which similar the characteristics of nanovesicles. Additionally, microscopy techniques (TEM and SEM) characterize the surface morphology, shape and size of the particles (**Figure 22**).

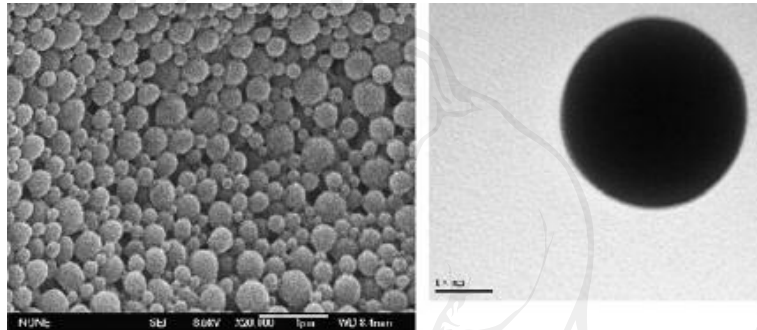


Figure 22 SEM and TEM images of PLGA nanospheres (Chen et al., 2009)

D. Applications of nanoparticulate delivery systems

Nowadays, the nanoparticles are widely used in drug delivery. The aims for nanoparticle entrapment of drugs are to enhance the stability and delivery to the target cells as well as the reduction the toxicity of the free drug. Some of companies have developed nanoparticles for drug delivery such as Advectus Life Science Inc. (polymeric nanoparticles to carry anti-tumor drug), NanoCarrier Co., Ltd (micellar nanoparticles to encapsulate drugs, protein and DNA) and Alnis Biosciences, Inc. (biodegradable polymeric nanoparticles) (Salata, 2004). For peptides and protein, several studied have demonstrated that nanoparticles can enhance the oral bioavailability of the

encapsulated therapeutic peptides and proteins (**Table 9**). Not as extensively as oral delivery systems, the nanoparticles have also been studied for transdermal delivery. Poly (ϵ -caprolactone) nanoparticles have been reported to increase the availability of octyl methoxycinnamate within the stratum corneum of 3.4 times when compared with the OMC emulsion, although the use of nanoparticles did not appear to increase skin permeation (Alvarez-Roman et al., 2004). It has investigated the topical application of chitosan-based nanoparticles containing plasmid DNA (pDNA) as a potential approach to genetic immunization (Cui et al., 2001).

1.4.8 Biological assay of scar treatment

1.4.8.1 *In vitro* biological assays to evaluate scar treatment

A. Antioxidative activity

There is evidence that immunological and biochemical changes are associated with thermal injury, including pyridinoline crosslinks which are present in large quantities in hypertrophic scar. It has been reported that free radicals are associated with the formation of pyridinoline (Wan et al., 1999). The antioxidant would be beneficial for treating scarring by free radical scavenging.

DPPH free radical scavenging activity assay: DPPH (1,1-diphenyl-2-picrylhydrazyl), a stable free radical, has been widely used to monitor the free radical scavenging abilities (the ability of a compound to donate an electron) or hydrogen donating activities of various compounds. DPPH, a radical generating substance, has a deep violet color due to its unpaired electron. Free radical scavenging ability can be followed by the loss of the absorbance as the pale yellow non-radical form is produced

Table 9 Studies on various nanoparticles to enhance oral bioavailability of the therapeutic peptides and proteins (Rieux et al., 2006)

Peptides/ proteins	Polymer used to prepared	Size (nm)	Observations/results
Insulin	Poly(isobutylcyanoacrylate)	300	Decreased of glycaemia from 300 mg/dl to a normal level of 125 mg/dl
Insulin	Poly(isobutylcyanoacrylate)	400	High variability in the concentration of insulin crossing the intestinal barrier, and the absence of modification of the glycaemia
Humalog®			
Insulin	Poly(fumaricanhydride)/poly (lactide co-glycolide)	<1 µm	Maintained normoglycaemia in the face of a glucose challenge
Insulin	Chitosan	270-340	Insulin doses of 50 U/kg and/or 100 U/kg were effective at lowering the glycaemia of diabetic rats
Insulin	Chitosan-glucomannan		Delayed hypoglycemic response at 14 h post administration maintained for >10 h.
Calcitonin	Chitosan-coated PLGA	200-300	Reduced blood calcium over 12 h after administration of the NP at doses of 125 IU/kg and 250 IU/kg.
Calcitonin	PEG-chitosan	160-250	Chitosan-PEG nanocapsules enhanced and prolonged the intestinal absorption of salmon calcitonin. 0.5 % PEG-CS>1% PEG-CS>CS coating>PEG coating=lipidic nanoparticles
Cyclosporin A	Chitosan HCL	100-150	1.8-folds increase of AUC when compared with Neoral® microemulsion
Cyclosporin A	Poly(methacrylic acid and methacrylate) copolymers: Eudragit® E100, L100, L100-55 & S100	37-107	Bioavailability increased (32.5% to 13.6%) compared with the Neoral® microemulsion
Dalargin	Tween 80 and PEG 20000 coated poly (butylcyanoacrylate) (PBCA-NDSs)	100	Analgesia with double-coated PBCA-NDSs compared to single-coated PBCA-NDSs (either Tween 80 or PEG)
mEpo DNA	Chitosan	70-150	Rapid increase of hematocrite, sustained for a week

The reaction of the DPPH radical in the presence of the antioxidant compound during the DPPH assay is shown in **Figure 23**. The DPPH radical scavenging assay became a reference point to evaluate the *in vitro* antioxidant capacity since it is a simple, rapid and sensitive method (Locatelli et al., 2009).

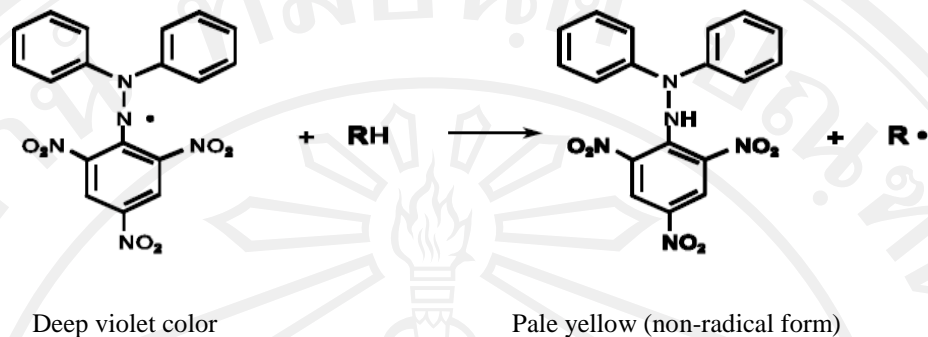


Figure 23 Reaction of the DPPH radical in the presence of the antioxidant during the DPPH assay (Prakash, 2001)

Lipid peroxidation inhibition assay: Lipid peroxidation is the oxidative deterioration of polyunsaturated lipids and it involves ROS and transition metal ions. The ferric thiocyanate (FTC) method is one of the peroxide values determination. The FTC method was used to measure the amount of peroxide at the beginning of lipid peroxidation, in which peroxide will react with ferrous chloride and form ferric ions. Ferric ions will then unite with ammonium thiocyanate and produce ferric thiocyanate. The substance is red, and denser color is indicative of higher absorbance (Aqil et al., 2006).

The antioxidant activities of the rice endosperm protein hydrolysate have been reported (Zhang et al., 2009). The Neutrased hydrolysate from rice endosperm protein (NHREP) took on DPPH radical scavenging activity similar to α -tocopherol. The percentage inhibition of autooxidation in the linoleic acid system by NHREP was 82.09%, similar to that of α -tocopherol (86.59%) on day 5 at the same concentration (Figure 24).

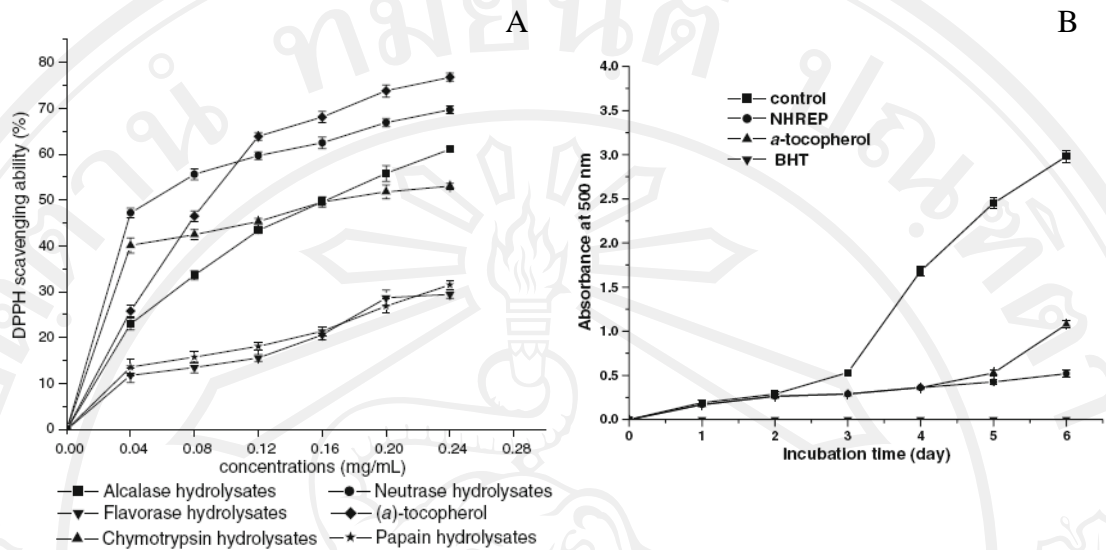


Figure 24 (A) DPPH radical scavenging activities of various hydrolysates from the defatted rice endosperm protein (REP) and (B) Inhibition of linoleic acid autoxidation by the Neutrased hydrolysate from rice endosperm protein (NHREP)

B. Cytotoxicity on human skin fibroblast

In recent years, dye exclusion test is a rapid method to assess cell viability. This method is based on the principle that live cells possess intact cell membranes that exclude certain dyes, such as trypan blue, eosin, or propidium, whereas dead cells do not. The stained and unstained cells are counted with a standard light microscope or flow cytometer. The most widely use of colorimetric techniques are the tetrazoline (MTT) and sulforhodamine B (SRB) assays. The MTT assay is based on the metabolic reduction of colorless tetrazolium salt, by mitochondrial enzyme activity in viable cells, to formazan salt (blue), which can be quantified spectrophotometrically. It is particularly useful for assaying cell suspensions because of its specificity for living cells.

However, the MTT assay is not linear with cell number at high cell densities, cell-line differ in their ability to reduce the dye. The protein-binding dye sulforhodamine B (SRB) is used for instead of MTT. The SRB assay is based on the measurement of cellular protein content. After an incubation period of the cells treated with the samples in 96-well plate, cell monolayers were fixed with 10% (w/v) trichloroacetic acid and stained for 30 min, after which the excess dye was removed by washing repeatedly with 1% (v/v) acetic acid. The protein-bound dye was dissolved in 10 mM Tris base solution for OD determination at 510 nm using a microplate reader (Vichai et al., 2006). This method does not only allow a large number of samples to be tested within a few days, but also requires only simple equipment and inexpensive reagents. The SRB assay is therefore an efficient and highly cost-effective method for screening. In addition, the SRB appeared to be more sensitive than the MTT assay, with a better linearity with cell number and higher reproducibility (Keepers et al., 1991). Economides et al. have compared the cytotoxic effect of resilon which is a new material that is a candidate to replace gutta-percha as a core root filling material against two fibroblast cell lines, L929 (mouse skin fibroblasts) and RPC-C2A (rat pulp cells) by SRB assay. Cytotoxicity in a descending order was the following: Resilon>Roeko gutta-percha>Dentsply gutta-percha. The cytotoxicity of Resilon increased significantly from 24 h to 48 h in both cell lines (Economides et al., 2008). Representative photographs of cells are shown in **Figure 25**.

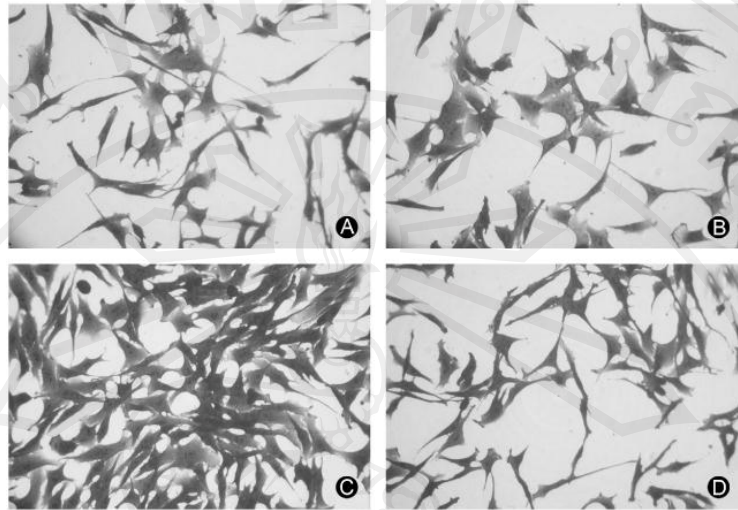


Figure 25 Representative photographs of cells (original magnification x100). A=Control L929 cells at 24 h; B=L929 exposed to Dentsply gutta-percha for 24 h; C=Control RPC-C2A cells at 48 h; D= RPC-C2A exposed to Resilon for 48 h (Economides et al., 2008).

C. Gelatinolytic activity on MMP-2 stimulation (zymography)

Matrix metalloproteinases (MMPs) are a family of calcium-dependent, zinc-containing endopeptidases that are structurally and functionally related (Sternlicht et al., 2001). They are secreted in an inactive (latent) form, which is called a zymogen or a pro-MMP. These latent MMPs require an activation step before they are able to cleave extracellular matrix (ECM) components. Their latency is maintained by an unpaired cysteine sulfhydryl group near the C-terminal end of the propeptide domain. This sulfhydryl acts as a fourth ligand for the active site zinc ion, and activation requires that this cysteine-to-zinc switch be opened by normal proteolytic removal of the propeptide domain. The thiol group is replaced by a water molecule that can then attack

the peptide bonds of MMP targets. The family of human MMPs consists of 23 different forms that are divided into 6 groups (**Table 10**).

Table 10 Types of MMPs (Beurden et al., 2005)

Subgroup	MMP	Name	Substrate
1. Collagenases	MMP-1	Collagenase-1	Col I, II, III, VII, VIII, X, gelatin
	MMP-8	Collagenase-2	Col I, II, III, VII, VIII, X, aggrecan, gelatin
	MMP-13	Collagenase-3	Col I, II, III, IV, IX, X, XIV, gelatin
2. Gelatinases	MMP-2	Gelatinase A	Gelatin, Col I, II, III, IV, VII, X
	MMP-9	Gelatinase B	Gelatin, Col IV, V
3. Stromelysins	MMP-3	Stromelysin-1	Col II, IV, IX, X, XI, gelatin
	MMP-10	Stromelysin-2	Col IV, laminin, fibronectin, elastin
	MMP-11	Stromelysin-3	Col IV, fibronectin, laminin, aggrecan
4. Matrilysins	MMP-7	Matrilysin-1	Fibronectin, laminin, Col IV, gelatin
	MMP-26	Matrilysin-2	Fibrinogen, fibronectin, gelatin
5. MT-MMP	MMP-14	MT1-MMP	Gelatin, fibronectin, laminin
	MMP-15	MT2-MMP	Gelatin, fibronectin, laminin
	MMP-16	MT3-MMP	Gelatin, fibronectin, laminin
	MMP-17	MT4-MMP	Fibrinogen, fibrin
	MMP-24	MT5-MMP	Gelatin, fibronectin, laminin
	MMP-25	MT6-MMP	Gelatin
6. Others	MMP-12	Macrophage	Elastin, fibronectin, Col IV
	MMP-19	metalloelastase	Aggrecan, elastin, fibrillin, Col IV, gelatin
	MMP-20	Enamelysin	Aggrecan
	MMP-21	XMMP	Aggrecan
	MMP-23	CMMP	Gelatin, casein, fibronectin
	MMP-27	Epilysin	Unknown
	MMP-28		Unknown

The protease enzymes which are the family of matrix metalloproteinase (MMPs) and involved in extracellular matrix (ECM) degradation have been shown to play the key role in collagenolytic activity. The hypertrophic scars and keloids are associated with the reduction of MMPs. The expression of MMPs was reduced in

psoriatic keratinocytes with hyperproliferative keratinocytes (Philips et al., 2010). Studies of fibroblasts from hypertrophic scars showed a decrease in mRNA expression or in activity of collagenase (Arakawa et al., 1996; Ghahary et al., 1996). Among MMPs, MMP-2 has been described to play an important role in the final degradation of the fibrillar collagens after the initial cleavage by collagenase. Gelatin zymography is mainly used for the detection of the gelatinases, MMP-2 and MMP-9, respectively (**Figure 26**). It is extremely sensitive because the levels of 10 pg of MMP-2 can already be detected (Kleiner et al., 1994). Zymography is an electrophoretic technique used to identify proteolytic activity in enzymes separated in polyacrylamide gels under nonreducing conditions. Both active and latent forms of MMP-2 and MMP-9 can be measured by zymography, because the zymography process (a denaturation of the enzyme for the electrophoresis and a renaturation before incubation for activity determination) activates various unfolded proenzyme forms. However, only active form can be degrade the collagens of hypertrophic scars.

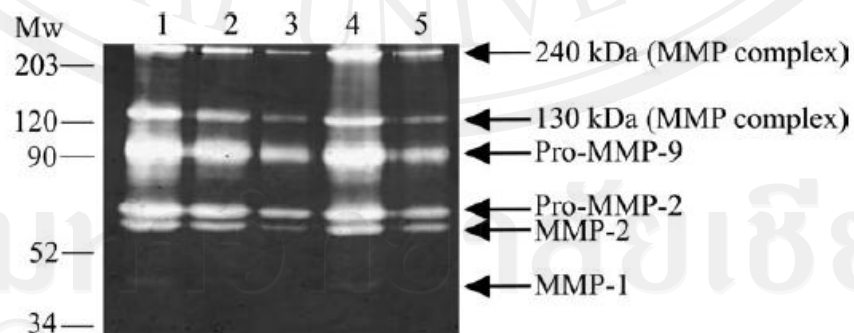


Figure 26 Gelatin zymography (Beurden and Hoff, 2005)

D. Collagenolytic activity

The measurement of collagenolytic activity by Moore and Stein (1954) was widely used. This method is based on the use of a modified ninhydrin reagent for the photometric determination of amino acids and the related compounds. The principle of this assay is the formation of a purple compound when ninhydrin reacts with the free alpha amino acids. The reaction is carried out after the addition of the enzyme solution to the substrate (collagen and gelatin) in Tris-HCl buffer (pH 7.5). The reaction is stopped by adding trichloroacetic acid. The amino acid in the supernatant is determined by ninhydrin test. The concentration of the hydrolyzed amino acids is determined by a standard curve based on a solution of L-leucine. One unit (U) of the enzyme activity is defined as the amount of enzyme required for the hydrolysis of 1 μ mole of substrate per min. Several studies have determined the collagenolytic activity by the method of Moore and Stein, such as collagenase from the Mackerel (*Scomber japonicas*) (Park et al., 2002), protease from the filefish (*Novodon modestrus*) (Kim et al., 2002) and serine protease from the viscera of sardinelle (*Sardinella aurita*) (Hayet et al., 2011). Collagenase activity was estimated by the method of Gross and Lapiere (1962) which is a simple method and requires no special materials or equipment. Small drops of sample were placed into holes made in the collagen gel and incubated at 37°C in a moist atmosphere of 10% CO₂-90% O₂. The collagenase activity was estimated after 24 and 48 h of incubation by measuring the diameter of lysis caused by the digestion of the gel.

This method has been used to evaluate collagenase activity of enzymes from microbials.

34 strains of *Pseudomonas aeruginosa* showed the collagenase activity whereas 38 strains of *Escherichia coli* were not activity (Wellisch et al., 1984).

Alternatively, collagen degradation is evaluated using the three-dimensional extracellular matrix. Previous study has investigated the profile of plasmin-dependent and independent collagenolytic activity of murine skin fibroblasts. The 24-well plates were coated with collagen gel and fibroblasts were seeded in the center of each well and allowed to adhere for 8 h. Following washing, serum-free medium was added to each well with or without PDGF-BB, plasminogen, or protease inhibitors as indicated. After 5 d, cells were removed by trypsin/EDTA or detergent lysis and the remaining collagen film stained with Coomassie brilliant blue. The sites of collagen degradation were visualized as zones of clearing (**Figure 27**). The collagenolytic activity was observed under plasminogen-condition. Fibroblasts were stimulated with PDGF-BB in the presence of cysteine- (E-64d), aspartyl- (pepstatin A) or serine- (SBTI or aprotinin) proteinase inhibitors maintain collagenolytic activity (Sabeh et al., 2009).

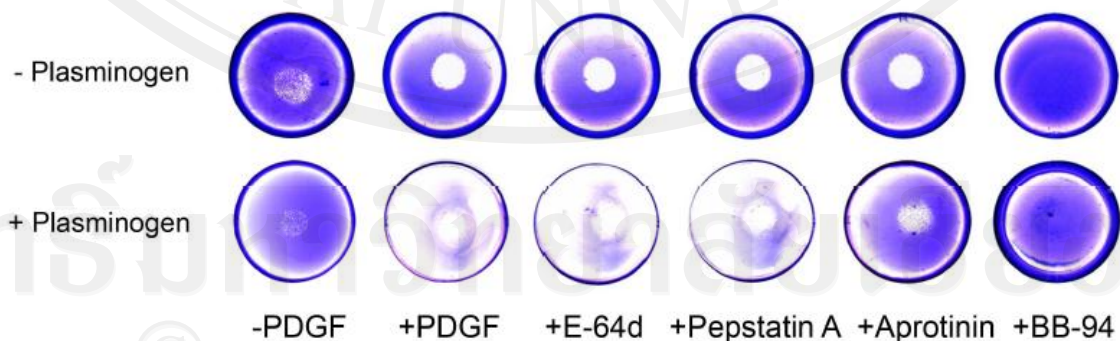


Figure 27 Profile of plasmin-dependent and independent collagenolytic activity of murine skin fibroblasts (Sabeh et al., 2009)

1.4.8.2 *In vivo* scar treatment evaluation assay

A. Rabbit skin testing for irritation

The evaluation of skin irritation potential is essential to ensuring the safety of individuals in contact with a wide variety of substances designed for industrial, pharmaceutical or cosmetic uses. Before using to human skin including scar treatment, the irritation evaluation of chemicals or formulations is necessary. The most common test is the rabbit skin irritation assay described in the OECD test guideline 404 and in the European Chemicals Bureau Annex V part B.4 (<http://ecb.jrc.it/testing-methods/>) which was initially described by Draize (Draize et al., 1944). Acute skin irritation can be evaluated *in vivo* on the shaved rabbit skin. The product is applied to the skin and the appearance of edema and/or erythema is evaluated at 1, 24, 48, and 72 h after application (**Table 11**). The scoring system enables products to be classified from nonirritant to very irritant (Vinardell et al., 2008). The skin irritation potential of the chemicals is often summarized as the 'primary irritation index' (PII) calculated from the erythema and edema grades according to the following formula: $PII = [(\sum \text{erythema grade at 24/48/72 h} + \sum \text{edema grade at 24/48/72 h}) / 3 \times \text{number of animals}]$. The irritation degree was categorized based on the PII values as negligible (PII = 0-0.4), or slight (PII = 0.5-1.9), moderate (PII = 2-4.9) or severe (PII = 5-8) irritation (Kamkaen et al., 2007).

Currently, the European Centre for the Validation of Alternative Methods (ECVAM) has supported formal validation studies on *in vitro* tests for predicting skin irritancy and corrosivity. Several reconstructed human epidermis models (EPISKINTM, SkinEthicTM and EpiDermTM) have been accepted for skin irritation testing. The samples

are put on the surface of the epidermis model. After incubation period, cell viability is assessed with the use of MTT colorimetric test. Eighteen cosmetic products were tested using EpiDerm™ and single 24-hour exposure at 100% concentration. The MTT assay results were compared to the results from skin irritation Draize testing using rabbits. The correlation coefficient between the *in vivo* and *in vitro* results was $r = -0.671$ (Genno et al., 1998).

Table 11 Draize evaluation of dermal reactions (Bashir et al., 2001)

Skin reactions	Score
<u>Erythema and eschar formation</u>	
No erythema	0
Very slight erythema (barely perceptible)	1
Well-defined erythema	2
Moderate to severe erythema	3
Severe erythema (beet redness) to slight eschar formations (injuries in depth)	4
<u>Edema</u>	
No edema	0
Very slight edema (barely perceptible)	1
Slight edema (edge of area well defined by definite raising)	2
Moderate edema (raised approximately 1 mm)	3
Severe edema (raised more than 1 mm and extending beyond the area of exposure)	4

The irritant properties of a new developed calcium phosphate ceramic, α -tricalcium phosphate (α -TCP) have been assessed after single application to the intact skin of the rabbit. The primary irritation index (PII) of α -TCP was no significant toxicity/irritability (PII = 0.0), while positive control (98% lactic acid) did cause

significant skin irritation ($PII = 2.11$) (Kojic et al., 2009). It has been demonstrated that gel containing solid lipid nanoparticles of vitamin A was nonirritant to the skin with no erythema or edema and gave primary irritation index of 0.00 (Pople et al., 2006).

B. Rabbit ear model for hypertrophic scar and keloids

determination

The etiology of hypertrophic scarring in humans has the three factors including genetic predisposition, delayed epithelialization, and wound tension. The animal model of hypertrophic scarring in the rabbit ear has been shown to be similar to the human condition in histologic and visual appearance with respect to larger wounds, response to steroids, and improvement in degree of scarring with the advanced age. For the rabbit ear model for hypertrophic scar and keloids determination, the hypertrophic scars were created down on the ventral side of the ear of the New Zealand White rabbits using a dermal biopsy punch. The perichondrium overlying of the ear cartilage was carefully removed, which delays epithelialization of the defect, supporting hypertrophic scar formation. The effect of the treatment can be compared using the scar elevation index (SEI), which is the measure of the height of the raised, hypertrophic scar as the ratio of the central-most scar area to the same area of the normal surrounding skin (**Figure 28**), with an SEI of 1 suggesting no raised height of the scar.

The previous study has been demonstrated that the treatment with different concentrations of oleanolic acid for 22 days significantly inhibited hypertrophic scarring in rabbit ear tissue. The hypertrophic scarring was significantly inhibited in a dose-dependent manner (2.5%, 5% and 10%) in the treatment groups, with the mean SEIs of

2.63±0.20, 2.12±0.32 and 1.87±0.24, respectively (Wei et al., 2011). It has determined the effectiveness of treating scars with microporous paper tape or silicone gel sheeting (SGS) in preventing hypertrophic scarring. No difference in mean SEI between treatment groups was seen (paper tape group=1.32; SGS group=1.41 and control=1.35) (Tollefson et al., 2012).

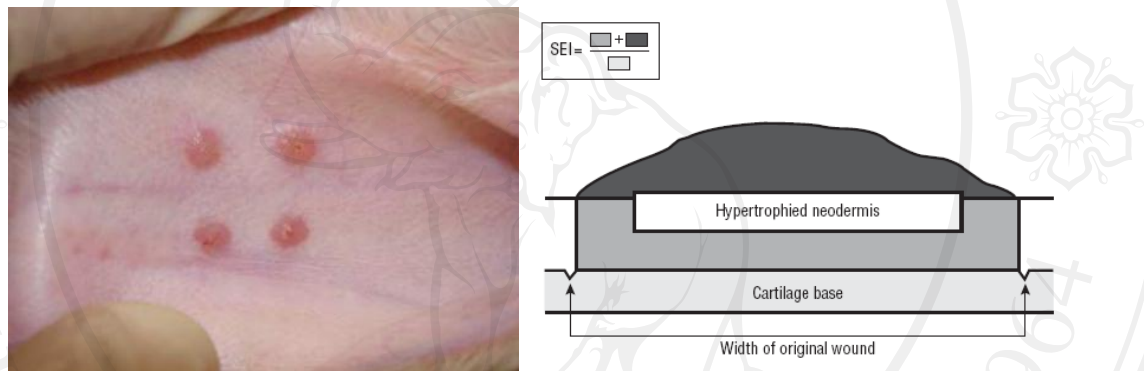


Figure 28 Hypertrophic scar in the rabbit ear model and the scar elevation index (SEI) evaluation (Tollefson et al., 2012)

The red Duroc pig was described as a model of hypertrophic scarring nearly 30 years ago. This model had appeal owing to the similarity of porcine skin to human skin (Zhu et al., 2007). The wounds were created with a Padgett dermatome (surgical instrument) on the backs of 7-week-old female, red Duroc pigs. The wounds were allowed to granulate and re-epithelialize without application of topical agents or dressings and were photographed at the times of biopsy. The histological of biopsies from wounds was evaluated under light microscope. The increased numbers of

myofibroblasts, mast cells and collagen nodules were present in Duroc scar similar to human hypertrophic scar (Harunari et al., 2006).

C. Performance test of scar reduction in human volunteers

The skin irritation safety testing and risk assessment is a critical requirement before human exposure. A clinical scar assessment in human is considered suitable for the comparison of clinical results when it is tested as reliable, feasible, consistent, and valid. Various scar assessments are available by clinical assessment and visual assessment scores. The outcome of scar improvement represents in the scar flatness by measuring the maximum vertical elevation of the scar above normal skin by a dial caliper. Scar erythema and elasticity are measured using a Mexameter and Cutometer, respectively. At present, the Vancouver scar scale is the most frequently used scar assessment scale (**Table 12**). For, a total score ranges from 0 to 14, whereby a score of 0 reflects normal skin.

Table 12 The Vancouver scar scale (Draaijers et al., 2004)

<u>Vascularity</u>		<u>Pigmentation</u>	
Normal color	0	Normal color	0
Pink	1	Hypopigmentation	1
Red	2	Mixed pigmentation	2
Purple	3	Hyperpigmentation	3
<u>Pliability</u>		<u>Height</u>	
Normal	0	Normal (flat)	0
Supple	1	<2mm	1
Yielding	2	<5mm	2
Firm	3	>5mm	3
Banding-rope like tissue	4		
Contracture	5		

The clinical response of keloidal and hypertrophic scars was compared after the treatment with intralesional triamcinolone acetonide (TCA) alone or combined with 5-fluorouracil (5-FU), 5-FU alone, and the 585-nm flashlamp-pumped pulsed-dye laser (PDL). Five segments of each scar were randomly treated with the 4 different regimens. All hypertrophic portions of the treated segments showed significant flattening compared with the baseline and control segments in all patients (**Figure 29**). The degree of scar erythema was significantly reduced at week 32 (12 weeks after the sixth treatment) at the laser-irradiated segments, at week 16 (2 weeks after the eighth injection) at the 5-FU-treated and control segments, and at week 24 (2 weeks after the tenth injection) at the TAC+5-FU-treated segments (Manuskiatti et al., 2002).



Figure 29 Hypertrophic median sternotomy scar at week 0 (A) and week 32 (B). A, Pulsed-dye laser-irradiated segment. B, Triamcinolone acetonide-treated segment. C, 5-fluorouracil-treated segment. D, Triamcinolone acetonide- and 5-fluorouracil-treated segment. E, Control segment (Manuskiatti and Fitzpatrick, 2002)